UNIVERSITY OF CALIFORNIA
RIVERSIDE

Atmospheric Nitrogen Deposition Changes Microbial Nitrogen Cycling in Desert Soils

A Dissertation submitted in partial satisfaction
of the requirements for the degree of

Doctor of Philosophy

in

Microbiology

by

Hannah Baer Shulman

September 2022

Dissertation Committee:
Dr. Emma Aronson, Chairperson
Dr. Jason Stajich.
Dr. Peter Homyak.

The Dissertation of Hannah Baer Shulman is approved:

_____

_____

_____

Committee Chairperson

University of California, Riverside

Acknowledgements

I would like to thank my dissertation advisor, Dr. Emma Aronson, for her support and mentorship over the past 6 years. Thank you Emma for encouraging me to be an independent and curious researcher, for supporting me in chasing all the incredible opportunities I've had during the course of my PhD, and for teaching me to never stop swimming. Thank you to the members of my committee: Dr. Jason Stajich and Dr. Pete Homyak, for your invaluable feedback and support on both my dissertation research and overall graduate education. Jason – you have taught me so much about genomics and bioinformatics both through your classes and our conversations, for which I am eternally grateful. Pete – thank you for being both a joy and a rock during grueling fieldwork days and for your enthusiasm and curiosity about my research.

Thank you to the members of the Aronson lab both past and current: Dr. Mia Maltz, Keshav Arogyaswamy, Dr. Brooke Pickett, Dr. Denise Jackson, Dr. Chelsea Carey, Dr. Yang Yang, Hannah Freund, Talyssa Topacio, Vanessa Montellano, and Mark Swenson. Thank you all for providing a supportive and collaborative research environment, and especially for sticking together during the weird days of the pandemic. Thank you to my undergraduate mentee, Natalie Tam, for her help with bench work and the positive energy she brought to the lab with her excitement about microbiology.

This dissertation project was a highly collaborative research effort and I have to thank all the groups that helped me both at UCR and other institutions. Huge thanks to Dr. Darrel Jenerette, and to the members of the Jenerette and Homyak labs including Dr. Alex Krichels, Dr. Jennifer Eberwein, Dr. Holly Andrews, and Aral Greene. Thank you to all the wonderful folks at Northern Arizona University who took the time to train me in

molecular methods including Dr. Lela Andrews, Dr. Michala Hayer, Dr. Ben Koch, and Dr. Egbert Schwartz. Thank you so much to the isotope group at Lawrence Livermore National Lab and especially to Dr. Steven Blazewicz for giving me the amazing opportunity to collaborate with the national laboratory and take my research to a whole new level. I cannot thank Dr. Mike Allen and Dr. Edie Allen enough for all their help during my time at UCR and for being essentially bottomless wells of wisdom.

I am so grateful for all the other great people I met at UCR including Dr. Michala Phillips, Dr. Courtney Collins, Dr. Teresa Bohner, Dr. Kelley Clark, Dr. Claudia Castro, Danielle Stevenson, and Dr. Sandra Armengol Vall. Thank you all for being my associates in both friendship and science. Thank you so much to all my amazing family who supported me through this long process and were always my cheerleaders. I want to especially thank my two wonderful grandfathers, James Poulette I and Dr. Foster Brown. Thank you to my mom, Paula Shulman, for being my #1 fan and always believing in me. And last but undeniably not least, thank you to my amazing partner, Dr. Sören Weber, for being my co-conspirator in all things, for benevolently helping me with my statistical modeling, for keeping me caffeinated, and for being my north star when I feel lost at sea.

Funding was provided by the University of California, Riverside Department of Microbiology & Plant Pathology, from the UCR Center for Conservation Biology through the Shipley Skinner Endowment award, from the Department of Energy SCGSR program, and from the University of California Office of the President through the Lab Fees Fellowship. Additional support came from the National Science Foundation and Joshua Tree National Park.

ABSTRACT OF THE DISSERTATION

Atmospheric Nitrogen Deposition Changes Microbial Nitrogen Cycling in Desert Soils

by

Hannah Baer Shulman

Doctor of Philosophy, Graduate Program in Microbiology
University of California, Riverside, September 2022
Dr. Emma Aronson, Chairperson

Microbial nitrogen cycling in hot desert soils is dominated by bursts of biogeochemical metabolic activity during short periods of water availability. Both edaphic traits of the soil ecosystem and the functional traits of the soil microbiome influence the transformation of nitrogen during this process. The aim of this research is to determine how soil bacteri and fungi transform mineral N and how air pollution in the form of atmospheric nitrogen deposition (N-dep) impacts nitrogen cycling. I used a set of desert field sites across a nitrogen deposition gradient in order to investigate soil microbiomes with increasing exposure to chronic atmospheric N-dep. In Chapter 1, I track bacterial and fungal communities over time in response to N addition to show patterns of community change corresponding to NO emissions. In Chapter 2, dry soils were taken from across the N-dep gradient and incubated with $^{15}NH_4$ in the lab in order to stimulate nitrogen assimilation by soil bacteria. Using this heavy isotope substrate enriched nitrogen assimilating bacterial DNA with ^{15}N, allowing me to determine the degree of

growth using DNA-quantitative stable isotope probing (DNA-qSIP). I then sequenced the bacterial 16S ribosomal gene from this qSIP-processed DNA and analyzed the sequence data to calculate isotope incorporation by each bacterial species. I found that with increasing exposure to N-dep, there was a more phylogenetically diverse group of assimilators. Furthermore, assimilation of NH4 across the N-dep gradient was dominated by 5 bacterial orders: Rhizobiales, Burkholderiales, Frankiales, Cytophagales, and Sphingomonadales. In Chapter 3, rewetting experiments were performed at 4 desert field sites with increasing annual loads of N-dep in order to stimulate bacterial metabolic activity. Metagenomes were sequenced in order to determine which nitrogen cycling functional genes were present in the soil, and which genes increase in abundance during rewetting. I found that N-dep significantly altered the composition of genes related to denitrification and organic matter decomposition, although I did not find any significant patterns of gene abundance before and after rewetting. Overall, these experiments demonstrate that nitrogen deposition alters several aspects of the desert nitrogen cycle by changing the composition and gene inventory of soil bacteria.

Table of Contents

List of Figures

List of Tables

Introduction

In hot desert systems, where plant and animal biodiversity is limited by oppressive heat and infrequent rainfall, resilient soil microbes are important drivers of biogeochemistry. However, there has been little mechanistic investigation into the contribution of desert microbes to total ecosystem processes. Anthropogenic activities and climate change may be driving the expansion of desert ecosystems, which already make up one fifth of Earth's surface area (Pointing & Belnap 2012; Makhalanyane et al. 2015). Therefore, investigation into the drivers of desert soil microbial community composition and function are needed to understand how desert microbes will react to their changing habitat, and how those changes will impact biogeochemical cycling. Arid soils are also sensitive to other anthropogenic forces such a surface disturbance, which increase desertification by limiting nutrients available to plants and slowing decomposition (Belnap, 1995).

Although deserts are typically thought to be limited in nitrogen (N), organic matter, and moisture, these soils have the potential to produce high emissions of gases, including greenhouse gases, during rapid periods of biogeochemistry following rewetting, known as pulses. This is because the availability of nitrogen in desert soils changes over time and in response to rainfall: there is evidence that arid ecosystems may exhibit high N emission potential (Schaeffer et al. 2017; Homyak et al. 2017; Leitner et al. 2017). Some of the highest globally reported pulses of nitrous oxide (N_2O) come from desert soil (Eberwein et al., 2020). A greater understanding of the microbial processes producing N_2O is needed to understand the variability of N_2O fluxes (Butterbach-Bahl et al., 2013). While the microbial genes that produce N gases have

been mostly well described on the mechanistic level, the composition of those genes in an ecosystem, the species they belong to, and how they operate under different soil conditions is needed to understand what factors are driving the expression of those genes and the subsequent production of N_2O and and other nitrogen oxides including nitrogen dioxide (NO_2) and nitric oxide (NO), collectively referred to as NO_x.

Furthermore, as climate change is predicted to increase the interannual variability of monsoonal events, there is a need to understand how microbes respond to rainfall events in the dry period, which would typically be without rain for months on end. Changing rainfall patterns have the potentially to dramatically alter desert soil stocks of C and N: deserts can hold dramatically more organic carbon as was seen when irrigation of desert soil associated with agricultural land use change led to up to 500% increases in SOM and increased N_2O loss (Trost et al., 2013).

Downwind of urban ecosystems, nitrogen deposition (N-dep), mostly in the form of NH_4 and NO_3 is a stress on arid soils, and may increase invasive grasses and fires (Fenn et al., 2003, 2010; Rao et al., 2009). Furthermore, arid soils receive among the highest rates of N-dep worldwide (Fenn et al., 2008). The desert ecosystems downwind of the Los Angeles urban area receive nitrogen deposition at loads of up to 25 kg per hectare per year. The impact of N-dep on the soil microbiome has been studied intensively, and established to have global patterns of decreased microbial biomass and respiration (Zhang et al., 2018). A mechanistic understanding of how atmospheric deposited nitrogen oxides influence microbial biogeochemistry is needed. Nitrogen deposition and nitrogen emissions are linked, as global emissions of N_2O are continuing to increase, likely due to nitrogen fertilization of agricultural soils and increased denitrification by fungi and bacteria (Thomson et al., 2012).

Both soil bacteria and archaea are capable of emitting N gases to the atmosphere through two respiratory processes: denitrification and ammonia oxidation. Denitrification begins with the dissimilatory reduction of NO_3 to nitrite (NO_2-) which can then volatize to gaseous nitrogen dioxide NO_2. There are at least three different clades of nitrate reductase enzyme, which is a widely phylogenetically distributed trait in bacteria (González et al., 2006). The reduction of nitrite to nitric oxide is also widespread through archaea and bacteria, especially in the Proteobacteria (Maia & Moura, 2014). Notably, not all nitrite reductase enzymes produce nitric oxide: for example several clades within the Bacteroidetes lineage contain the *nrfA* gene which converts nitrite to ammonia in a mechanism that competes with denitrification (Mohan et al., 2004). Denitrifiers then produce N_2O from NO using 2 clades of nitric oxide reducing protein (Stein, 2011, 2017).

Bacteria and archaea use ammonia monooxygenase to oxidize ammonia to hydroxylamine as a form of chemolithotrophic respiration. Hydroxylamine is then further oxidized to nitric oxide, nitrite, and nitrate. These bacteria use ammonia available in alkaline soils and are also capable of mineralizing ammonia from nitrogenous organic matter. Bacterial ammonia oxidizers belong to the beta and gamma proteobacterial clades, including species of Nitrosomonas and Nitrosospira (Kowalchuk & Stephen, 2003). Bacteria from the monophyletic clade Nitrospira are also capable of ammonia oxidation (Koch et al., 2019). Ammonia is hypothesized to be fully oxidized to nitrate in more oxic conditions and only partially oxidized to nitrite or nitric oxide when oxygen is limited (Kuypers et al., 2018).

Fungal denitrification was first identified in Fusarium oxysporum (Shoun & Tanimoto, 1991), which contains the genes to produce nitrate reductase *narG* (NO_3 →

NO_2-) copper-containing nitrite reductase *nirK* (NO_2-→ NO) and cytochrome p450 (NO → N_2O). To date, no fungi have been demonstrated to produce N_2 from N_2O (Aldossari & Ishii, 2021). Notably, while fungal *nirK* is highly similar to bacterial *nirK* and hypothesized to have been acquired via endosymbiotic gene transfer (Kim et al., 2009; Timmis et al., 2004), fungal p450 is a unique and evolutionarily distinct entity (Vázquez-Torres & Bäumler, 2016). Unlike bacterial nor proteins which are membrane bound, fungal p450 nor is not localized to a mitochondrial membrane but soluble in both cytosol and mitochondria (Shoun et al., 2012). The diversity of fungal denitrifiers in soil systems has not been well described. Currently, 60 genera have been shown to contain denitrifying species with 90% of those in the Ascomycota phylum (Mothapo et al., 2015). Studies performed in soils with antifungal and antibiotic inhibitors suggest fungi contribute more to N_2O emissions relative to bacteria (Chen et al., 2014).

NO can also be produced by non-respiratory fungal processes involved with both inflicting and mediating nitrosative stress in plant-fungal and specifically plant-pathogen interactions (Cánovas et al., 2016). For example, the pathogen *Fusarium graminearum* releases NO when chemical signals of the plant host are detected and turn on the promoter for transcription of nitrate reductase (Ding et al., 2020). In this case, the hypothesized enzymatic source of NO is not a *nir* protein but flavohemoglobin NO dioxygenase (Marcos et al., 2016). In Aspergillus nidulans, oxidation of NO to NO_3 by flavohemoglobin proteins and assimilatory nitrate reduction are coexpressed as a strategy to detoxify large bursts of NO produced by plants (Schinko et al., 2010). Overall, the genes and proteins responsible for regulation of NO levels in fungi are not well understood, and have been studied in only a very limited number of model organism species. When considering the sources and sinks of N trace gases in the soil

ecosystem, it should be noted that since NO is toxic at the cellular level both plants and microbes have evolved systems to transform this molecule independent of respiration.

The potential microbial transformations of nitrogen described above also work in tandem with abiotic processes including chemodenitrification and co-denitrification to direct the flow of nitrogen. During co-nitrification, NO_2- and NO produced by microbial processes react with amine, imine, or azide organic compounds in the soil to produce N_2 or N_2O (Harris et al., 2021; Laughlin & Stevens, 2002; Shoun et al., 2012). The novel use of long read approach metagenome sequencing in tundra soil demonstrated for the first time that at the community level, denitrifying traits are spread across diverse bacterial species and very few taxa contained all the genes necessary for complete denitrification of NO_3 to N_2 or even N_2O (Pessi et al., 2020). While it has been estimated that more than two-thirds of N trace gas emissions arise from microbial denitrification and nitrification processes (Thomson et al., 2012), these processes interact with the soil matrix to produce N emissions through a combination of N-reducing enzymes, co- and chemo-nitrification.

In the following chapters, I will analyze desert soil microbial community composition, functional gene inventory, and growth on mineral nitrogen to address the following questions: 1) Does microbial community composition impact the emission of N trace gases? 2) How does chronic exposure to nitrogen deposition impact the ability of soil bacteria to assimilate nitrogen? 3) Does N-dep change the inventory of bacterial nitrogen cycling genes?

Chapter 1: Nitrogen pulses in two dryland systems: soil microbial processes and emissions.

Introduction

Respiratory pulses are key biogeochemical processes in arid ecosystems: During the dry summer period in arid ecosystems, soil organisms and plant life survive high temperatures and little rainfall. Over the course this "dry-down," labile forms of carbon (C) and nitrogen (N) accumulate in the top layer of soils through desiccation and photodegradation of soil organic matter (SOM) (Ma et al. 2012). Mineral N concentrations increase as plant N uptake is reduced and drought adapted microbes continually mineralize organic matter (Schaeffer et al. 2017). Labile compounds also persist as increasing hydrological disconnect across the soil compartment limits plant and microbial access to nutrients (Homyak et al 2016).

These long periods of low biological activity in the desert are punctuated by monsoonal events, when rainfall induces large pulses of biogeochemical activity resulting in soil emissions of CO_2 and N trace gases. In the wet winter period, higher soil moisture results in higher overall rates of above and belowground activity, but lower magnitude of emissions following rewetting. This is because these pulse processes are substrate limited, so conditions that increase the amount of labile nutrients (that is, the buildup of labile material during the dry period) result in higher emissions (Jenerette & Chatterjee, 2012). These rewetting induced pulses are an important part of desert biogeochemistry, and a single rewetting event is capable of releasing up to 10% of annual productivity (Unger et al., 2010; Lee et al., 2004).

Microbial transformations determine the fate of pulsed nitrogen: Once rewetting occurs, The oxygen (O_2) levels in the soil drops as water floods the soil matrix and O_2 is consumed during the following respiratory activity (Zaady, 2005) powered by the release

of mineral N, C and SOM from soil aggregates. The labile fraction of this SOM is understood to be a complex mixture of microbial osmolytes (N. Fierer & Schimel, 2003; J. Schimel et al., 2007), microbial necromass created during the dry-down (Blazewicz et al., 2014)), and highly decomposed plant biomass. Even deep horizon soil nutrients can be mobilized by frequent drying and rewetting cycles (J. P. Schimel et al., 2011).

Following rewetting, N is lost from the soil as trace gases in two phases. The first is an initial burst of N_2O and NO (Eberwein et al., 2020); (Leitner et al., 2017; Slessarev et al., 2021) occurring as quickly as 15 minutes post-rewetting. Mineral N is the most significant source of this pulse, although the amino acids in the organic nitrogen fraction are also transformed rapidly into N gasses. The mechanism generating this “fast phase” N is not clear. Theoretically, incomplete denitrification of NO_2- to NO and N_2O could rapidly result in high emissions. The NO_2-pool could be derived from the rush of solubilized NO_3 and NH_4 being metabolized by denitrifiers (Parker & Schimel, 2011) and autotrophic nitrifiers (Fierer & Schimel, 2002; Zhang et al., 2018), respectively. Studies show that reduced NO_3 is the source of fast phase pulses of N_2O in desert shrub and chaparral systems (Krichels et al., 2022) and NO in grassland systems (Slessarev et al., 2021). There is good evidence that this fast phase pulse is created by abiotic mechanisms: biotically produced NO_2- can interact with acidic clay mineral surfaces in the dryland soils, producing NO (Homyak et al., 2017) or N_2O (Harris et al., 2021) by chemodenitrification.

It is likely that abiotic mechanisms are driving the “fast phase” since transcript markers of microbial activity either slightly correlate or do not correlate with emissions (Placella, 2011; Vázquez et al., 2020). However, the current primer sets commonly used in these studies may provide an incomplete picture of N emitting processes (Frostegård

et al., 2020) A second, “slow phase” of NO is released over the course of hours to days following rewetting and is likely biotic in origin (Krichels et al., 2022; Slessarev et al., 2021). There is evidence the original substrate for this NO pulse is NH_4 (Homyak et al., 2016).

The ecological framework for microbial community responses to nutrient pulses: There are a number of soil bacterial and fungal processes potentially contributing to a bi-phasic pattern of N emissions from arid soils. There have been several studies looking for microbial evidence of pulsed N emissions by measuring functional gene abundance and expression: In desert soil crusts, denitrifying gene expression drives NO and N_2O emissions (Abed et al., 2013; Maier et al., 2022). In grasslands, the activity of the denitrifying genes explained “background” N_2O emissions outside of the drought/rewetting pulse, but didn’t have a clear relationship with pulsed N_2O emissions, which were heavily driven by soil pore water indicating an abiotic source of N_2O (Harris et al., 2021). Loss of nitrogen from grasslands may also be a result of the ratio of genes for denitrification and dissimilatory nitrate reduction to ammonia, i.e., the competition between nitrogen conserving and nitrogen emitting processes (Putz et al., 2018).

While microbes with complete and/or well resolved denitrification inventories (e.g. *Fusarium oxysporum* or *Bradyrhizobium japonicum* (Bedmar et al., 2005)) are rare, evidence suggests that NO_3, NO_2-, or NO transformation capability is broadly distributed across phylogenetic lineages. Therefore, I predict that phenological patterns of N emissions will correlate with changes in microbial composition as rewetting activated taxa respiring NO or N_2O grow and other taxa die off (Blazewicz et al., 2014). The aim of this experiment is to track soil microbial communities and soil emissions over time following a rewetting event in order to determine the microbes living in these soils, their

responses to rewetting, and look for evidence of specific taxa contributing to pulsed emissions of N.

Emissions were measured and microbial communities were sampled before rewetting and at 4 post-rewetting timepoints. This experiment was performed at a low elevation desert site with higher emission potential and higher elevation pinyon juniper forest site with lower emission potential to capture variation in magnitude of rewetting response. I analyzed both fungi and bacteria in order to determine the relative contribution of these two populations to emissions. Lastly, I analyzed bacterial activity (growth on $H_2{}^{18}O$) during rewetting in the desert site to gain additional insight into bacterial change over time and more accurately determine which taxa were capable of growth and metabolism. My hypotheses for this experiment are:

1. At both sites, changes in the soil microbiome over time will peak with peak soil respiration 4-8 hours post rewetting, characteristic of the "slow phase" of N emissions. In some desert soils, there is high spatial heterogeneity of microbial communities, with more variation across space than time, however post-rewetting events are an exception (Armstrong et al., 2016). Therefore, I will analyze both the compositional similarities of each post-rewetting timepoint (i.e., search for set of shared taxa that grow in response to rewetting) and compositional changes from pre-rewetting (i.e., quantify change representing growth and death of taxonomically distinct, but functionally redundant taxa). Analysis of microbial composition over time is difficult due to noise introduced by sequencing technologies, relic DNA, spores, and spore-like dormant "seed microbes" among other things (Coenen et al., 2020; Ridenhour et al., 2017;

Shade et al., 2013). Therefore, I also used quantitative stable isotope probing to determine which bacteria were definitively active in order to complement my time series analysis.

2. Post rewetting, the forest site will have lower emissions due to higher fungal dominance over soil microbial processes. It has been established that lower available labile substrates result in lower emission at Santa Rosa. Soil nutrient conditions are both created by and select for fungal over bacterial processes, and therefore there will be more fungal community change over time at Santa Rosa.
3. N addition will increase emitted N at both sites through its selection for N-limited, N emitting bacterial taxa. I expect that bacterial community changes will be correlated with N emissions and likewise N addition will impact composition. Echoing prior results, which show mineral nitrogen selects for bacterial over fungal metabolism, I expect fungal responses to be suppressed and bacterial responses increased.

Methods

Study sites: This experiment was performed at two sites near Palm Springs in southern California: Both sites have been previously described in depth (Chatterjee & Jenerette, 2011; Jenerette & Chatterjee, 2012). 1) Boyd Deep Canyon (BDC), a desert scrub site dominated by *Larrea tridentata* and sandy textured soils with a pH of 7.9, mean annual precipitation of 23.6 cm, 1.6% soil organic matter, and elevation of 289 meters. 2) Santa Rosa Peak (SR8), an evergreen forest site dominated by *Pinus jeffreyi* and Sandy loam soils with a pH of 6.1, mean annual precipitation of 132 cm, 8.8% soil organic matter, and elevation of 2489 meters. Climatic patterns at both sites are Mediterranean with the majority of rain events in the winter season and the occasional summer monsoonal event. This work was carried out at the end of July 2016, corresponding to the end of the seasonal dry period. This year also saw relatively higher levels of rainfall comparable to historic rainfall following years of extreme drought (Griffin and Anchukaitis 2015).

Simulation of soil rewetting and tracking emissions: 6 plots were established at each site. At both sites the plots were located under the creosote bushes (Boyd Canyon) or pinyon pines (Santa Rosa peak) to capture N dynamics in the biogeochemical hotspots occurring in the shrub or tree's island of fertility (Chatterjee & Jenerette, 2011). Two sets of PVC collars were installed at a depth of 10cm. Each set included two 25 cm diameter collars and two 10 cm diameter collars. The first set of collars was rewet with a control treatment of sterile H_2O equivalent to a 2cm rain event. The second set was rewet with the same volume of water with H_4NO_3 equivalent to 30 kg N ha- 1 (n=6). Rewettings were performed in the morning before 12pm.

CO_2, NO, and N_2O gas emissions were tracked using a custom array of gas analyzers similar to the setup in (Andrews & Jenerette, 2020; Eberwein et al., 2020). CO_2 measurements were made on the 10cm collars using a closed-chamber system (LI-8100A; LI-COR Bioscience, Lincoln, NE, USA; Fig. 1). NO and N_2O measurements were collected simultaneously from the 25cm collar using an open-chamber system as described in (Eberwein et al., 2020). To quantify each flux, concentrations of CO_2, N_2O, and NO were measured every 1, 1, and 10 secounds, respectively, for approximately 5 minutes inside the sealed chambers. Initially NO_2 was also measured, but concentrations were small compared to NO so measurement was discontinued for the full measurement period. Fluxes were quantified at 5 timepoints: before rewetting treatments were applied (Pretreatment), 15 minutes, 4 hours, 8 hours, and 24 hours post rewetting.

Soil collection and nucleic acid extraction: Soils sampled from the top 5 cm were collected at the 5 timepoints described above. Soil sampling equipment was sterilized between each collection with 80% EtOH to prevent contamination between plots. Soils were stored on ice while the study was conducted and then stored at -20C for DNA extraction. DNA was extracted using soils from a subset of the plots (n=3) with the Qiagen PowerSoil Powerlyzer kit following manufacturer's instruction with the addition of a heated lysis step (65C x 25 minutes) to improve yields from dry, low biomass soils.

Marker gene sequencing: To target bacterial communities, the V3 region of the 16S rRNA gene was amplified from soil DNA extracts using the 515F (5'-GTGCCAGCMGCCGCGGTAA-3') and 806R (5'-GGACTACVSGGGTATCTAAT-3') primer set. DNA was amplified using KAPA HiFi HotStart ReadyMix (Roche Diagnostics, Indianapolis, IN, United States) and 0.2 μM of each primer. The reaction was carried out

with the following thermocycle: Initial denaturing at 95°C for 3 minutes, followed by 25 cycles of 95°C for 30 seconds, 55°C for 30 seconds, 72°C for 30 seconds, and concluding with a final extension at 72°C for 5 minutes. To target fungal communities, the internal transcribed spacer 2 (ITS2) region was amplified from soil DNA extracts using the 5.8S-F (5'-AACTTTYRRCAAYGGATC WCT-3') /ITS4-FunR (5'-AGCCTCCGCTTATTGATATGCT TAART-3') primer set (Taylor et al. 2016). DNA was amplified using the Phusion High Fidelity Master Mix (NEB), an additional 3mM MgCl2, and 0.2 μM of each primer. The reaction was carried out with the following thermocycle: Initial denaturing at 95°C for 2 minutes, followed by 35 cycles of 95°C for 30 seconds, 55°C for 30 seconds, and 60°C for 4 minutes. Libraries were indexed and then sequenced with paired ended 300bp reads on the Illumina MiSeq platform at the University of California, Riverside Genomics Core.

Marker gene bioinformatics: Demultiplexed 16S sequences were analyzed in QIIME2 (Bolyen et al., 2019). After visualizing read quality profiles in QIIME2, forward and reverse reads were trimmed to 279 and 260 base pairs, respectively. DADA2 was then used to remove chimeras, quality filter, and sort reads into amplicon sequence variants (ASVs). 16S sequences were assigned taxonomy with a bayesian classifier using reference sequences from the SILVA database release 132 (Quast et al., 2013). ITS2 reads were processed using the amptk bioinformatics pipeline (Palmer et al., 2018). Briefly, USEARCH9 was used to merge paired-end reads, cluster sequences, and pick ASVs. ASVs were assigned taxonomy using the amptk custom ITS2 database and hybrid taxonomy assignment algorithm. For both 16S and ITS2 datasets, data from a negative sequencing control was used to remove <10 contaminant ASVs. Due to low

read counts 3 bacterial samples were removed from the data. Any ASV that made up less than 0.005% of total relative abundance were removed (Bokulich et al., 2013). After processing and filtering, there were a total of 3907 bacterial and 2463 fungal ASVs.

Modeling and statistical analysis: Ordination was used to visualize the effects of Site, timepoint, and nitrogen treatment on microbial community composition. Ordination of microbial communities was performed by principal component analysis of aitchison distances on ANCOM-BC transformed abundances (Lin & Peddada, 2020a) to account for effects of read depth. PERMANOVAs were then used to determine the significance of factors on community composition. Taxonomic patterns were examined by analyzing the average relative abundance of replicate shrubs (n=3). ANOVAs were used to determine the impact of time, site, and nitrogen treatment on both instantaneous flux rates and cumulative fluxes of CO2, N2O, and NO. ANOVAs were determined if microbial beta and alpha diversity metrics were significant drivers of both instantaneous flux rates and cumulative fluxes. To explicitly model microbial beta diversity and gas data together, subplot-specific distances between each time point and pretreatment were decomposed into turnover (species replacement) and nestedness (species loss) using the betapart function (Baselga & Orme, 2012) in order to calculate community change over time. Both species richness and evenness were additionally calculated at each time point. For bacteria, I also included phylogenetically weighted metrics of beta diversity (weighted unifrac distances) and alpha diversity (faith's phylogenetic diversity) in the models. In all ANOVA models, error terms were hierarchically ordered to account for site, then shrub, then collar (synonymous with nitrogen treatment). Microbial metrics that were found to significantly predict variation of flux data were then further analyzed with linear regression. All analyses were performed in R.

DNA quantitative stable isotope probing: Dry soils were collected from the top 5cm of soil beneath 3 shrubs at Boyd Deep Canyon in early September 2018, at the peak of the dry season. 3 grams of dry soil were incubated with 1.2 uL $H_2{}^{18}O$ or natural abundance H_2O controls (n=3) for 7 days in sterile screw top falcon tubes on the lab bench. DNA was extracted from 0.2g of soil incubations as described above and stored at -80C until further processing. For each sample, DNA equal to a total weight of 1ug was combined with 3.6mL saturated CsCl solution in a 3.3-mL OptiSeal ultracentrifuge tube. The samples were spun in an OptimaMax benchtop ultracentrifuge using a Beckman TLN-100 rotor at 127,000 x g for 72 h at 18°C. After centrifugation, each sample was split into approximately 24 fractions of 200 uL using a Harvard apparatus pump 33 and the Beckman fractionation recovery system. The refractive index (RI) of each fraction was measured with a Reichert AR200 digital refractometer and converted to density using the following equation: density = RI*10.995-13.73. The DNA fractions were then purified from the CsCl solution using isopropanol precipitation. The fractions within the density range of 1.65200-1.72000 g/mL were used to move forward with qPCR and sequencing. There were a total of 7 fractions per sample within this range. I used qPCR to determine copies of the 16S rRNA gene in each density fraction. Triplicate 10 uL reactions included: 1 uL of template DNA, 0.25 uM of each primer (388F, 5'-GCTGCCTCCCGTAGGAG-3' and 518R 5'-ATTACCGCGGCTGCTGG-3',), Forget-Me-Not EvaGreen qPCR Master Mix (Biotium), and 1.5mM $MgCl_2$. Reactions were performed on a CFX384 Touch Real-Time PCR Detection System (Bio-Rad Laboratories) using a program of 95°C for 2 min followed by 40 cycles of 95°C for 30 s, 64.5°C for 15 s, and 72°C for 15 s. All reactions had an efficiency > 85% and R2 > 0.9990. Samples were then prepped for sequencing the 16S gene using the 515F/806R

primer set, sequenced on the Illumina MiSeq, and analyzed in QIIME2 as described above. Excess atom fraction caused by incorporation of the ^{18}O was then calculated following the protocol outlined in (Hungate et al., 2015) and is summarized in the Supplementary Table 1.

Results

Tracking trace gas emissions following rewetting, and the impact of nitrogen addition:

I analyzed 2 different aspects of the flux data: a) the instantaneous flux rate calculated by measuring emissions for 5 minutes, and b) the total cumulative flux for each of the four post-rewetting timepoints (i.e. Pretreatment-15 minutes, Pre-4 hours, Pre-8 hours, and Pre-24 hours) determined by trapezoidal integration of instantaneous flux rates over time.

CO_2: Instantaneous CO_2 flux rates peaked 15 minutes post rewetting (Fig. 1.1) and this was different between sites [F=17.807, p=6e-5] with higher post rewetting flux rates at Boyd Canyon compared to Santa Rosa Peak. These results reiterate previous studies demonstrating that there is a higher magnitude of birch effect soil respiration in desert compared to forest sites (Jenerette & Chatterjee, 2012). CO_2 flux rates were elevated for the remaining 3 timepoints over the next 24 hours but were not significantly different between sites. In total there was an average of 7.2e5 ∓ 3.2e5 ug/m^2 and 5.7e5 ∓ 1.4e5 ug/m^2 of C-CO_2 emitted over 24 hours at Boyd Canyon and Santa Rosa Peak, respectively (Fig. 1.1). Nitrogen treatment did not affect the instantaneous flux rate of CO_2 or any measure of cumulative CO_2 emissions.

NO: There were observably different emissions patterns of NO between Boyd and Santa Rosa (Fig. 1.1), with site being the largest driver of instantaneous flux rates [F=33.406, p=1e-7] and cumulative emissions [F=72.371, p=1e-12]. At Santa Rosa, instantaneous flux rates were highest 15 minutes post-rewetting and fell to background rates seen before rewetting by 4 hours. At Boyd Canyon, there was not a spike in

emissions at 15 minutes post rewetting, but instead rates increased between 15 minutes and 4 hours and stayed elevated for the entire time course of the experiment. Nitrogen treatment only had a marginally significant impact on instantaneous flux rates [F=3.197, p=.08], but did significantly increase cumulative emissions of NO [F=5.241, p=.02]. At Boyd, 8.6e6 ∓ 3.2e6 ng/m^2 and 12.4e6 ∓ 5.6e6 ng/m^2 of N-NO were lost 24 hours after treating with water and nitrogen, respectively. At Santa Rosa, 0.7e6 ∓ 0.8e6 ng/m^2 and 1.5e6 ∓ 1.4e6 ng/m^2 of N-NO were lost 24 hours after treating with water and nitrogen, respectively.

N_2O: There was a large post-rewetting spike of N_2O emissions at Boyd Canyon, but virtually no N_2O emissions at Santa Rosa (Fig 1.1). At Boyd, fluxes peaked at 15 minute post rewetting but unlike the pattern seen for NO emissions, they fell back to pretreatment flux rates by 4 hours post rewetting. There was also a significant effect of nitrogen treatment on cumulative N_2O emissions [F=6.416,p=.01]: At Boyd Canyon, 3.8e3 ∓ 2.7e3 ug/m^2 and 2.3e3 ∓ 1.5e3 ug/m^2 of N-N_2O were lost 24 hours after treating with nitrogen and water, respectively.

Post-rewetting fungal and bacterial community changes:

Impact of treatment on bacterial community: I used PERMANOVA models to measure the combined effects of sampling site, nitrogen treatment, and time following rewetting on bacterial composition. As expected, site was the strongest predictor of the bacterial community [F=11.71, p=0.04](Fig. 1.2). This result was essentially an assumption of this experiment, as the two sites had significantly different plant communities. Nitrogen treatment also impacted composition [F=1.55, p=0.002], with

significant differences following rewetting with water alone versus water plus nitrogen. Additionally, there was an interaction between site and nitrogen treatment [F=1.55, p=0.002]. PCA analysis illustrates that there is limited overlap between nitrogen treated soil microbiomes and controls (Fig. 1.2). However, it is hard to say if one site had a stronger compositional response to nitrogen treatment: there is overall more beta dispersion at Boyd Canyon in nitrogen treated and control samples compared to Santa Rosa Peak.

Changes in bacterial composition over time: PERMANOVA analysis did not show that sampling time point was a significant predictor of composition or interacted with any other factors [F=0.91, p=0.93]. However, ordination methods are not ideal for detecting patterns of change over multiple time points due to autocorrelation of potentially functional redundant taxa within lower clades. Therefore, I analyzed distances alone to better isolate the within plot changes across the phenological series. While aitchison distances calculated using the ANCOM-BC algorithm were used for PERMANOVA and ordination analysis to best account for read depth affects, I additionally used weighted unifrac distance to determine phylogenetic changes, and sorensen distance decomposed into turnover (substitution of species in one sample by different species observed in other samples) and nestedness (elimination of species) in order to pick apart beta diversity patterns across time.

For bacteria, at both sites turnover values were higher than nestedness, indicating that most of the compositional changes over time were due to species substitution (Fig. 1.4). Neither nestedness nor turnover was significantly different over time at either site. However, while turnover was not affected by nitrogen treatment, nitrogen did significantly impact nestedness [F=10.284, p=0.003] and interacted with site

[F=5.318,p=0.03]. Specifically, nestedness was higher at all timepoints in the nitrogen treated shrubs (Fig. 1.4). Bacterial phylogenetic distances (PD) were also not significantly different over time, but there was an interaction between site and treatment of PD [F=7.037, p=0.01] with nitrogen treatment decreasing the phylogenetic changes over time at Santa Rosa Peak.

Impact of treatment on fungal community: Similar to bacterial communities, site was the biggest predictor of fungal composition [F=52.02, p=0.002] (Fig. 1.3), however comparing both the F means and PC axes between fungi and bacteria (Fig. 1.2, Fig. 1.3) indicates that this compositional difference was much greater in the fungal population. Nitrogen treatment also impacted post-rewetting fungal composition [F=4.86, p=0.002] and interacted with site [F=4.42, p=0.002]. Fungi at Boyd Canyon had a larger beta dispersion after nitrogen treatment compared to control, indicating that desert fungal composition was more responsive to nitrogen.

Changes in fungal composition over time: For fungal communities, turnover was generally higher than nestedness at Boyd Canyon but not Santa Rosa (Fig. 1.4). Fungal turnover was also overall lower compared to bacterial turnover. Turnover was not significantly different over time, but site and treatment had interacting effects on turnover [F=7.105, p=5e-7] with nitrogen decreasing fungal turnover at Boyd Canyon. Fungal nestedness was the only measure of microbial distance that was significantly different over time [F=3.221, p=0.01], peaking at 8 hours post-rewetting at Santa Rosa and continually increasing at Boyd Canyon (Fig. 1.4). Nitrogen also increased overall fungal nestedness at all timepoints [F=5.36, p=0.03]. I was not able to calculate unifrac distances due to the limitations creating phylogenetic trees using this marker gene region, so it is unknown how fungal phylogenetic patterns across compare to bacteria.

Taxonomic composition: To analyze the taxonomic differences between microbial communities at Boyd Canyon versus Santa Rosa Peak, I focused on composition of taxa before rewetting. At both sites, over 95% of the 2463 fungal ASVs classified at the Phylum level belonged to the Ascomycota, Basidiomycota, or Mucoromycota (Fig. 1.6). However, beyond the Phylum-level composition, the two sites had very different soil fungal communities. This is verified in the PCA analysis, where samples cluster by site along PC1, which accounts for 50.4% of variation in the microbial population (Fig. 1.3). Santa Rosa peak had proportionally more Basidiomycota and Mucoromyota, and a different class-level composition of Ascomycota. The desert soils of Boyd Deep Canyon notably had a high percentage (average ~40% relative abundance) of fungi belonging to the class Dothideomycetes.

Because the abundance of the Dothideomycetes was the clear distinguishing feature of the desert soils compared to forest soils, I then analyzed the genus-level patterns of relative abundances of this fungal class over time and in response to nitrogen treatment at Boyd Canyon (Supplementary Fig. 1.2). There were 12 genera of Dothideomycetes identified in these soils, with at least half of them including pathogenic species (Supplementary table 1.2). Notable and abundant genera include two species of the root pathogen *Pleiochaeta* and three species of the endoyphyte *Preussia,* which has been identified as an endophyte of creosote shrubs (Massimo et al., 2015).

Boyd Canyon and Santa Rosa peak had relatively more similar bacterial communities compared to fungal communities. PCA analysis shows that samples cluster by site along PC1, which accounts for 18.7 % of variation in the bacterial population (Fig. 1.2). At the Phylum level, both soils were dominated by Actinobacteria and Proteobacteria (Fig. 1.7). Santa Rosa had a high average relative abundance of

Acidobacteria while Boyd had a higher proportion of Chloroflexi. At both sites, bacteria belonging to the putative ammonia oxidizing order Nitrosomonadales and the putative NO producing order Nitrospirae were present at an average relative abundances ranging from .01-.1% (Supplementary Fig. 1.3), however due to the relatively low abundance of this clade I could not confidently analyze their change over time.

Modeling microbial dynamics and gas emissions: Bacterial nestedness had a significant positive correlation with cumulative CO_2 emissions (Fig. 1.5)[F=5.022, p=.03]. Fungal community structure also explained variation of cumulative CO_2 emissions, with fungal species richness a significant driver [F=5.623, p=0.03] and fungal nestedness a marginally significant driver [F=3.786, p=0.06] of cumulative CO_2 emissions. The evenness of the fungal community also predicted instantaneous CO_2 flux rates [F=4.606, p=0.01]. I found a significant correlation between cumulative NO emissions and composition of the fungal community (Fig. 1.5), with fungal nestedness [F=12.94, p=1e-3] and species richness [F=14.07, p=7e-4] explaining NO emissions over time. As expected, there is a significant interaction with Site [F=29.105, p=6.9e-6] as Santa Rosa did not have NO emissions after the initial large spike of NO seen at 15 minutes. Fungal nestedness was also marginally correlated to cumulative N_2O emissions [F=3.127, p=0.08], but overall there were no significant correlations between fungal composition and N_2O flux. No metrics of bacterial beta or alpha diversity were significantly correlated with instantaneous flux rates or cumulative fluxes of NO or N_2O.

Metabolically active bacteria in desert soil:

After filtering sequence data as described in the methods section, there were 3946 observed bacterial taxa. Of those, 511 were abundant enough across all fractions

and all replicates to calculate excess atom fraction, and of those 511, 262 taxa were defined as incorporators that grew on $H_2{}^{18}O$. Here we define an incorporator as a taxon with a bootstrapped minimum confidence greater than 0 as outlined in (Hungate et al., 2015). In summary, 6.6% of the observed taxa at Boyd Canyon were growing in significant numbers following rewetting. Out of those 262 incorporators, >75% belonged to one of three phyla (Fig. 1.8): Proteobacteria (101 incorporators), Bacteroidetes (69 incorporators), or Actinobacteria (32 incorporators). Excess atom fraction was also varied significantly between these three phyla [ANOVA F= 13.18, p=4e-6]: The Bacteroides had a mean excess atom percentage of 38%, the Proteobacteria 32%, and the actinobacteria had the lowest mean excess atom percentage at 18%. These results show that the majority of post-rewetting growth was carried out by only a small percentage of taxa across 3 phyla, although taxa belonging to 19 phyla were identified using 16S marker gene sequencing.

Discussion & Conclusions

Desert and forest soils emit different N trace gases in different patterns during rewetting response

At Santa Rosa peak, there was significantly less emission of both NO and N_2O compared to the desert. This was likely due to the forest soil having less labile organic matter and mineral N, and therefore less substrate for pulsed emissions (Jenerette & Chatterjee, 2012). While aspects of both fungal and bacterial composition were found to be significantly related to soil respiration of CO_2 and had a significant compositional response to N treatment, CO_2 emissions were not affected by N addition. These data suggest that total soil microbial respiration is not a nitrogen-limited process, but nitrogen addition may change the composition of respiring microbes.

The results found here do somewhat support my second hypothesis, that post-rewetting processes would be fungal dominated in forest soils: I did see a stronger pattern of increasing nestedness across time at Santa Rosa compared to Boyd. However, the difference in N emissions is more likely due to the difference in fungal composition between the desert and forest sites. In the desert, NO emissions were correlated with fungal compositional changes, not bacterial change as I originally predicted. In addition to taxonomic differences, the organic matter available to the soil fungi may be driving differences in N emissions: higher SOM in the forest soils could mean more available carbon to saprotrophs for fungal biomass synthesis. This may explain why carbon availability influences N losses from arid soils (Eberwein et al., 2015).

Bacterial change over time, noise, and nitrogen response

Post-rewetting compositional responses of soil microbiomes were difficult to detect with marker gene sequencing. While ordinations could identify significant responses to nitrogen treatments, change of communities over time were not similar enough to detect site level patterns of rewetting response. Decomposition of beta diversity into nestedness and turnover improved the understanding of soil microbiome change over time. Patterns of nestedness across ecological gradients indicate a correlation between species trails and environmental characteristics (Ulrich and Almeida-Neto 2012). While timepoint did not predict overall composition and composition could not predict instantaneous flux rates, nestedness of timepoints from pretreatment was significantly correlated to cumulative emissions, suggesting that functionally redundant clades at different shrubs carried out respiration processes. However, structural aspects of microbiome sometimes predicted flux, for example there were higher rates of instantaneous CO_2 emissions when bacterial and fungal composition was more evenly distributed.

Nitrogen addition did impact post rewetting bacterial composition but a correlation between total bacterial composition and N emissions could not be found, indicating that at the community level, most nitrogen limited bacteria are not contributing to pulsed N emissions. The results may suggest that bacteria are instead using the added nitrate as a source of N for biomass growth, and the compositional response seen in response to N addition represents soil bacteria capable of assimilatory nitrate reduction (Luque-Almagro et al., 2011; Ramond et al., 2022). These data do not rule out the possibility of bacterial denitrification or ammonia oxidation: there were ASVs belonging to the putative NO-producing nitrosomonad and nitrospira clades at both sites.

It is possible that these or other nitrate reducing microbes could be contributing to the "fast phase" pulse of NO (SR8) or N_2O (BDC) seen within 15 minutes of rewetting, either alongside or in tandem with abiotic processes.

Contrary to my 3rd hypothesis, the bacteria of Boyd Canyon responded at the community level to N addition but not correlated with NO or N_2O emissions. My exploratory study with $H_2{}^{18}O$ at Boyd showed that most of the actively growing taxa belong to 3 phyla. Two of those phyla, the Actinobacteria and Proteobacteria, were unsurprisingly active as they were also the most abundant in the 16S data. However, the Bacteroidetes phylum was disproportionately active compared to their relative abundance in the non-fractionated 16S data. These results reiterate that Proteobacteria and Actinobacteria are dominant in arid soils, and that the Chloroflexi, Planctomycetes, and Firmicutes may be disproportionately contributing to noise in 16S data.

Evidence for community-wide fungal production of NO in desert soil and the potential importance of plant-pathogen interactions

Out of all the data collected in this chapter, the strongest correlation between emissions and soil microbial change over time (Hypothesis 1) is between fungal nestedness and cumulative NO emissions in the soils at Boyd Canyon. At the community level, change in the fungal community is correlated in magnitude with losses of NO from the soil. These results suggest that fungal growth and death processes that produce changing composition are related to NO emissions and specifically, compositional changes due to loss of species. This mechanism could be happening if rewetting acts as a selective event on the fungal community, with certain taxa dying from osmotic shock and certain clades of taxa being able to increase in relative abundance.

Based on the taxonomic profiles of fungi present in Boyd vs. Santa Rosa, the fungal clade of Dothideomycetes is most likely to be responsible for producing any biotic NO emissions. This conclusion is based on the assumption that because the Dothideomycetes are the most abundant class of fungi at Boyd, and the most differentially abundant across the two sites, it is contributing to the difference in ecosystem output. Many of the fungal species and genera found in Boyd have been identified as plant pathogens in other environmental contexts, so it is possible that NO synthesis associated with plant-pathogen interactions could be resulting in NO emissions. Many species of the dothideomycetes have been confirmed to use NO in various secondary metabolism processes (Zhao et al., 2020). The abundance of apparent plant pathogens could be eliciting an NO burst from the shrubs or other plants growing under the shrub canopy (Kumar & Pathak, 2018), this seems unlikely as previous experiments in similar systems has shown that removing plants increases NO emissions (Homyak et al., 2016). Not all species of dothideomycetes are pathogenic, some species are non-pathogenic endophytes (e.g. *Preussia spp*., found in these soils (Massimo et al., 2015)) or saprotrophs (e.g. *Dictyosporium*). It was found that just a few clusters of function genes determine pathogenicity in this clade (Haridas et al., 2020). Future investigations into the potential role of fungal production of NO emissions from soil could benefit by targeting fungal NO producing genes including nitrite reducing p450nor (Higgins et al., 2016), or flavohemoglobin proteins involved in NO synthesis (Baidya et al., 2011). These genes may be producing NO as a part of respiratory denitrification, plant-pathogen interactions, or some overlap of the two processes (Cánovas et al., 2016).

These results also reiterate other recent findings that fungi, including pathogenic fungi are responsible for pulsed N in various ecosystems (Aldossari & Ishii, 2021; Chen et al., 2014; Huang et al., 2021; Laughlin & Stevens, 2002), although these studies are focused on production of fungal N_2O rather than NO. For example, (Huang et al., 2021) found that *Fusarium oxysporum*, a denitrifying species of fungi also found in these soils, was responsible for N_2O emissions in a fertilized agricultural soil environment.

In conclusion, this experiment supports that soil fungi are the primary microbial contributors to the "slow phase" of NO emissions following rewetting of desert soils. Specifically, fungi belonging to the Dothideomycetes are highly abundant in desert soil and may be driving N emissions, potentially through plant-pathogen interactions. Bacteria may be producing NO and N_2O in smaller amounts during either the slow or fast phase, as although community level correlation with emissions or flux rates was not found, we did identify the presence of putative ammonia oxidizers and denitrifiers in these soils. Furthermore, $H_2{}^{18}O$ qSIP of bacterial DNA shows that three phyla were most active after rewetting, supporting that our community composition data may be affected by persistent but non-active bacteria.

Figures & Tables

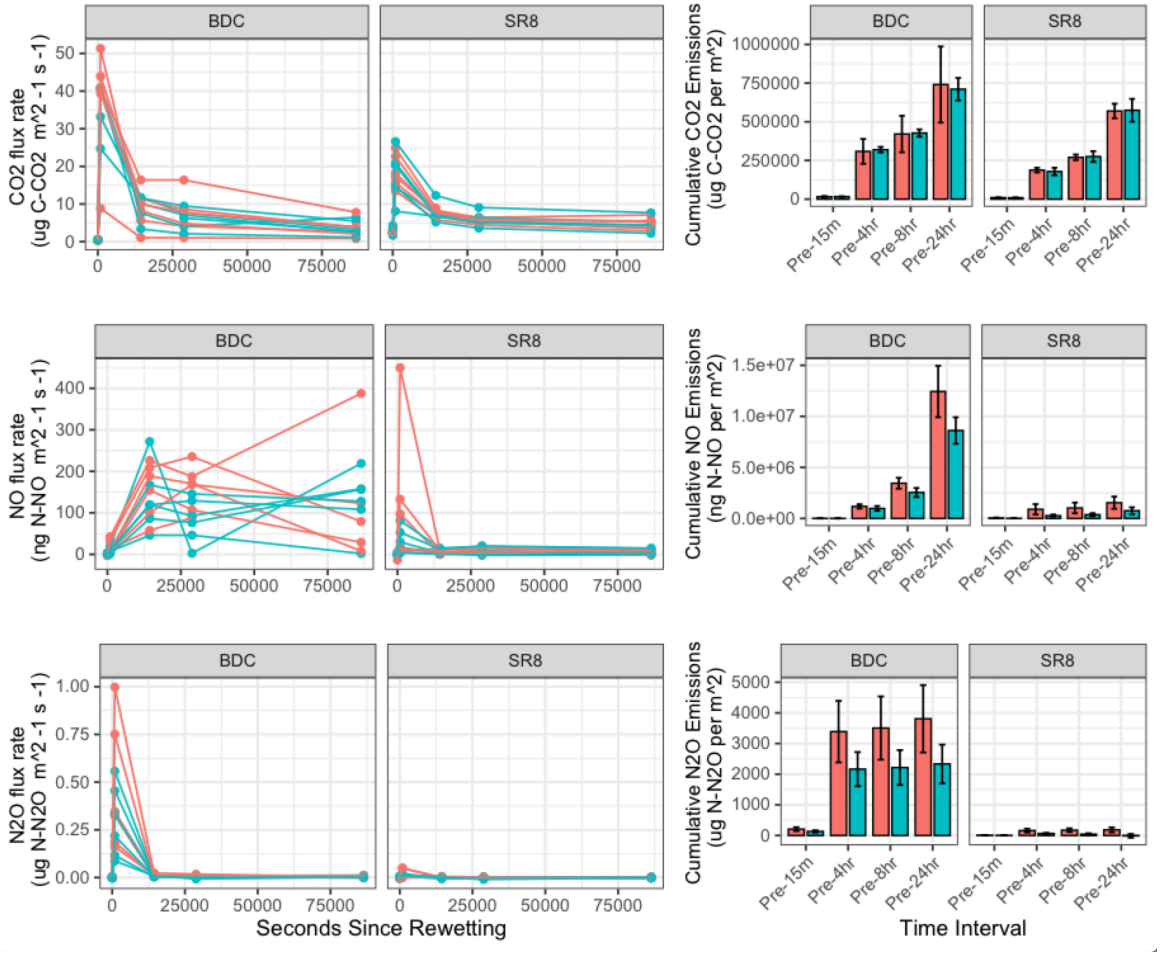

Figure 1.1: Post-rewetting emissions at two dryland sites: Instantaneous flux rates (left column) and cumulative emissions (right column) were measured at two dryland sites: a low elevation desert site, Boyd Deep Canyon (BDC) and a high elevation forest site, Santa Rosa Peak (SR8). Cumulative emissions at each timepoint were calculated by trapezoidal integration of all instantaneous flux rates (e.g. cumulative flux at 8 hours was calculated using the flux rates measured at Pretreatment, 15 minutes, 4 hours, and 8 hours). Soils were either rewet with water alone or nitrogen treatments. Scatterplot points of repeated measure instantaneous fluxes are connected by subplot (n=6). Bar Plots of cumulative emissions represent the mean and errorbars depict standard error of the mean.

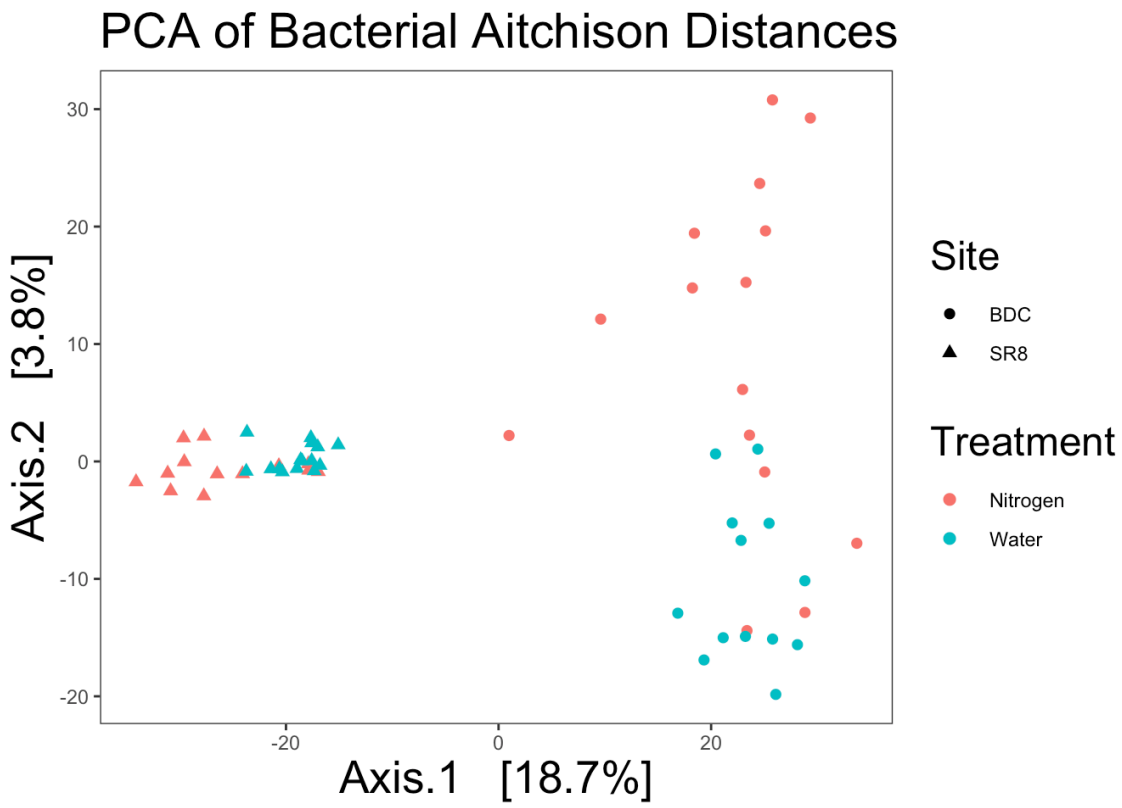

Figure 1.2: Bacterial Composition: Principal component analysis was performed on a euclidean distance matrix of ANCOM-BC normalized bacterial ASV abundances. Shape of points represents site, color represents treatment. Data for all 5 timepoints is shown but not differentiated.

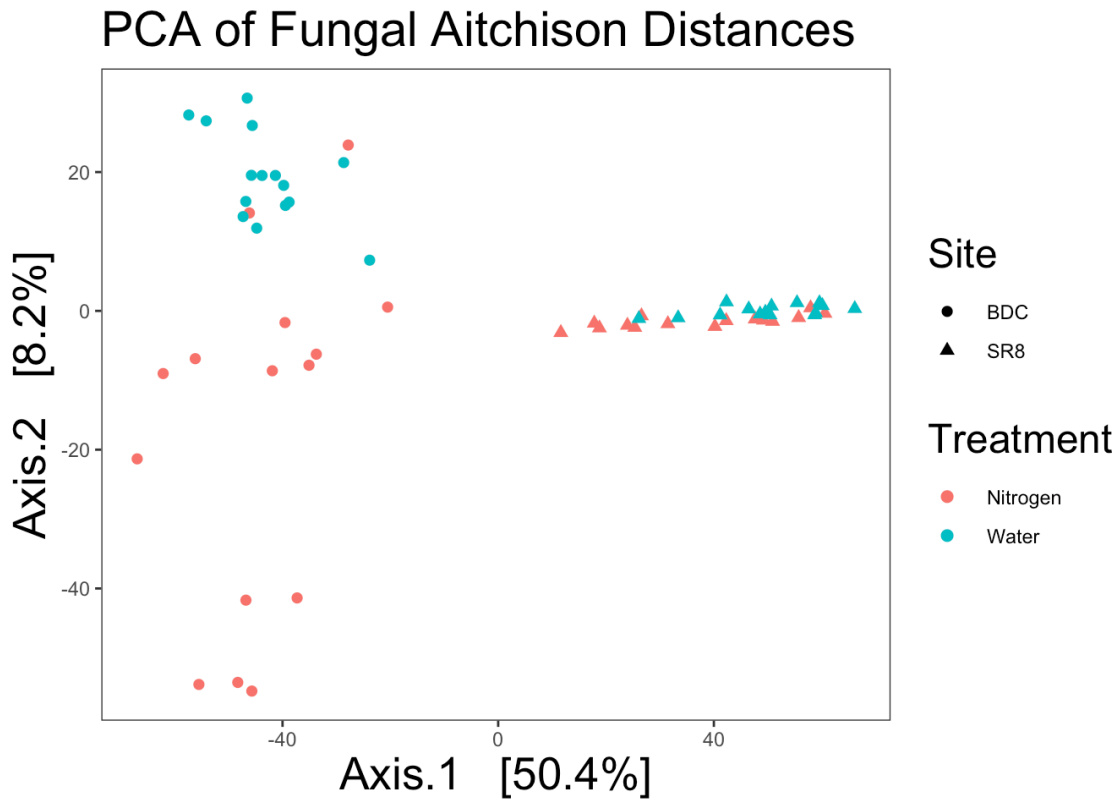

Figure 1.3: Fungal Composition: Principal component analysis was performed on a euclidean distance matrix of ANCOM-BC normalized fungal ASV abundances. Shape of points represents site, color represents treatment. Data for all 5 timepoints is shown but not differentiated.

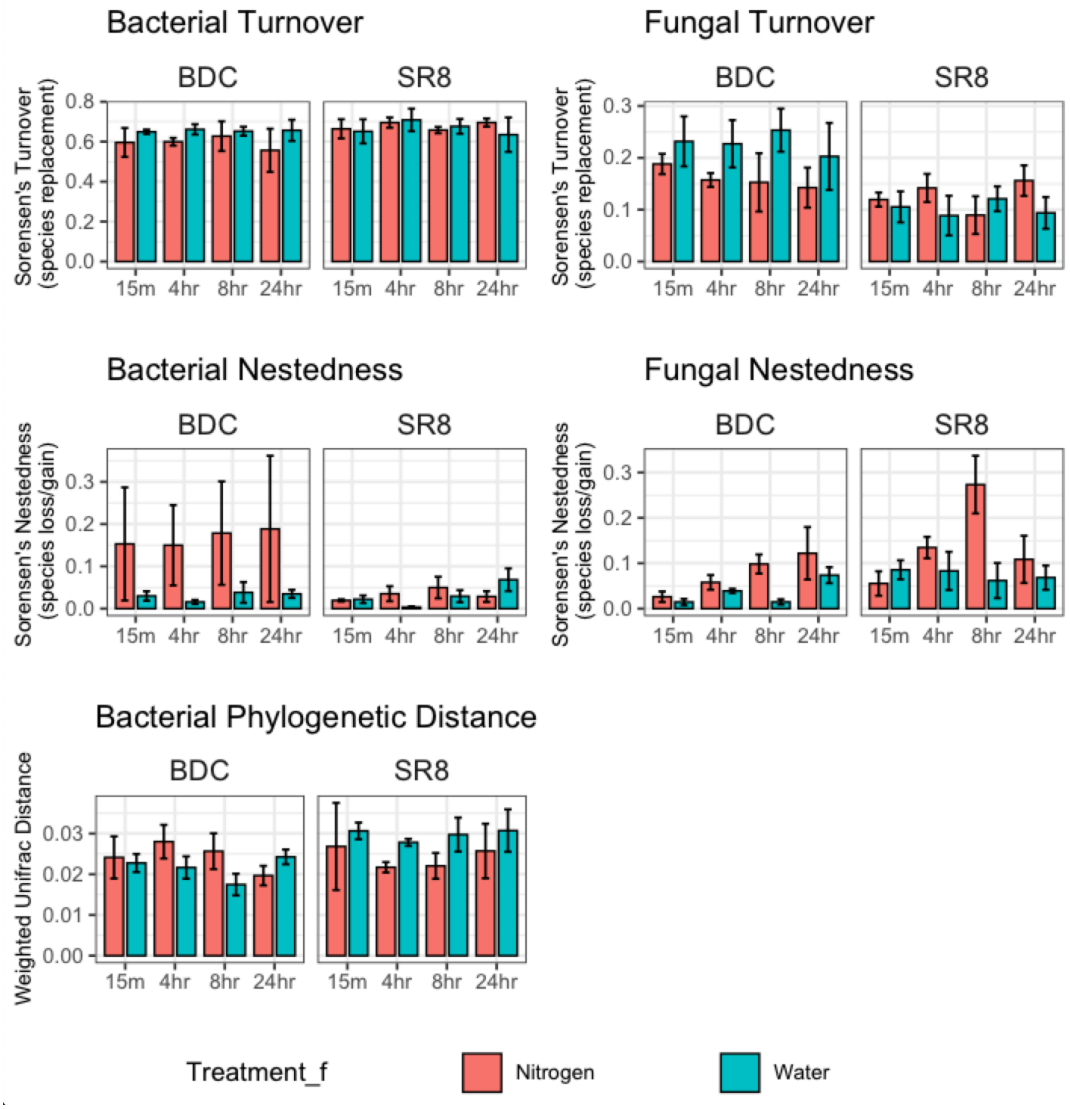

Figure 1.4: Decomposed beta diversity over time: The decomposed beta diversity metrics shown are the distance calculated between the pretreatment and timepoint indicated of each subplot (n=3). Errorbars represent the standard error of the mean. Turnover and nestedness were calculated from the Sorensen's index of filtered but non-normalized ASVs. Phylogenetic weighted unifrac distance was calculated from raw ASV counts.

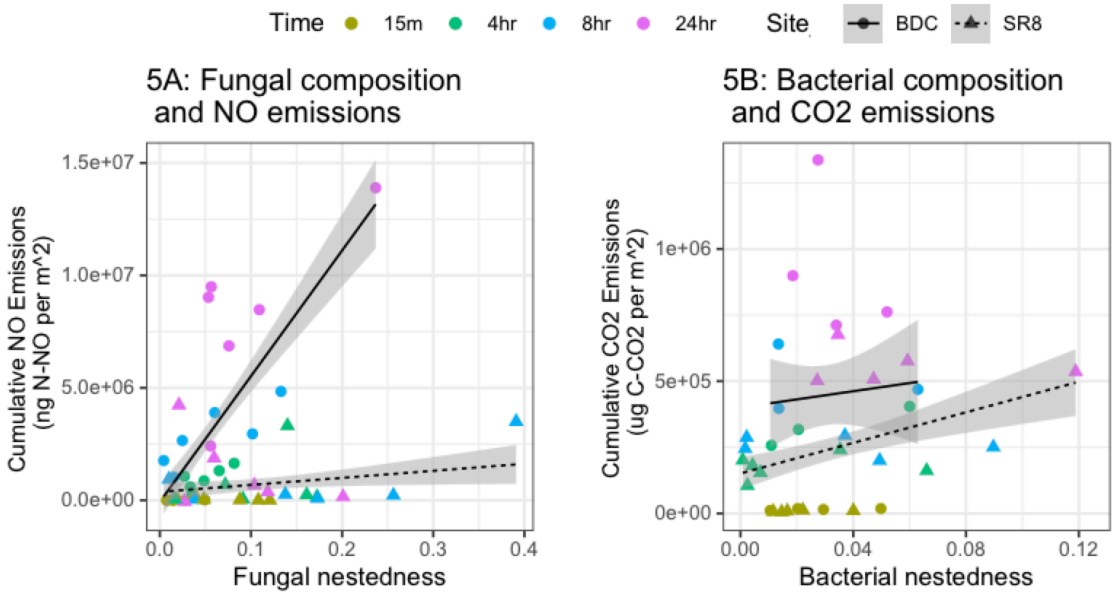

Figure 1.5: Correlation Between Microbiome Change Over Time And Cumulative Emissions: Scatterplot of subplot specific (n=3) nestedness (i.e. compositional distance due to species loss) and cumulative emissions from pretreatment. Timepoint is indicated by color. Regression lines represent linear regression for each site, gray area represents 1 standard error.

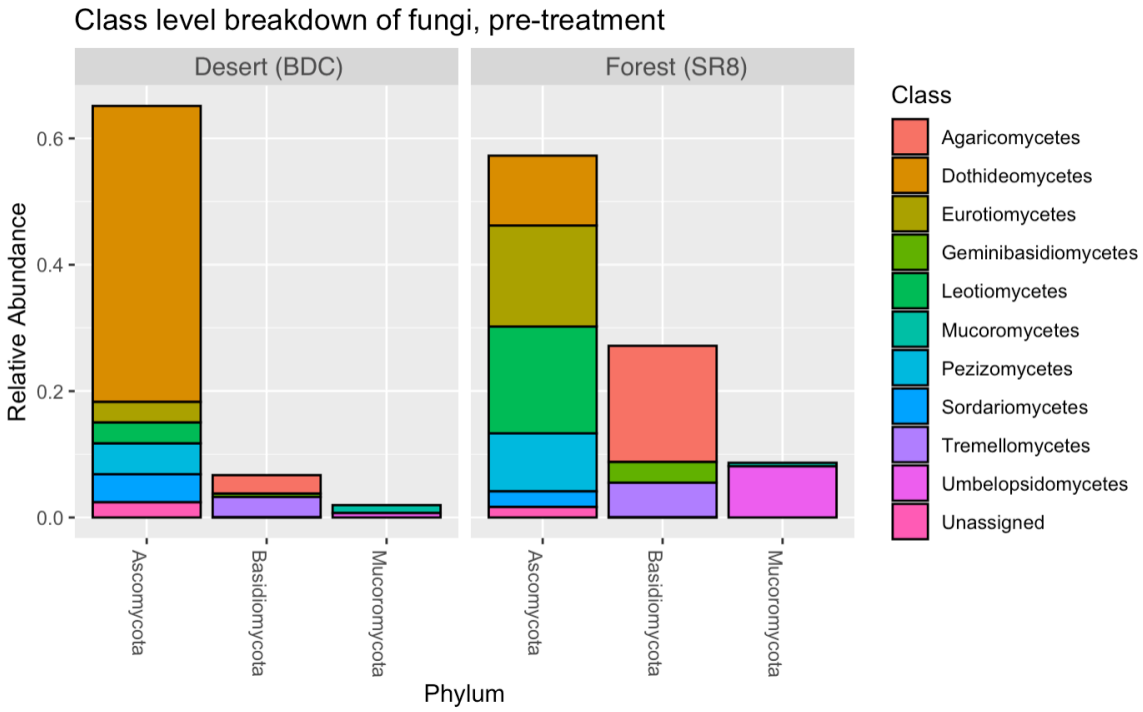

Figure 1.6: Comparison of fungal classes between sites: The average relative abundance of fungal classes in pretreatment soils at the desert site Boyd Deep Canyon (BDC) and the forest site Santa Rosa Peak (SR8).

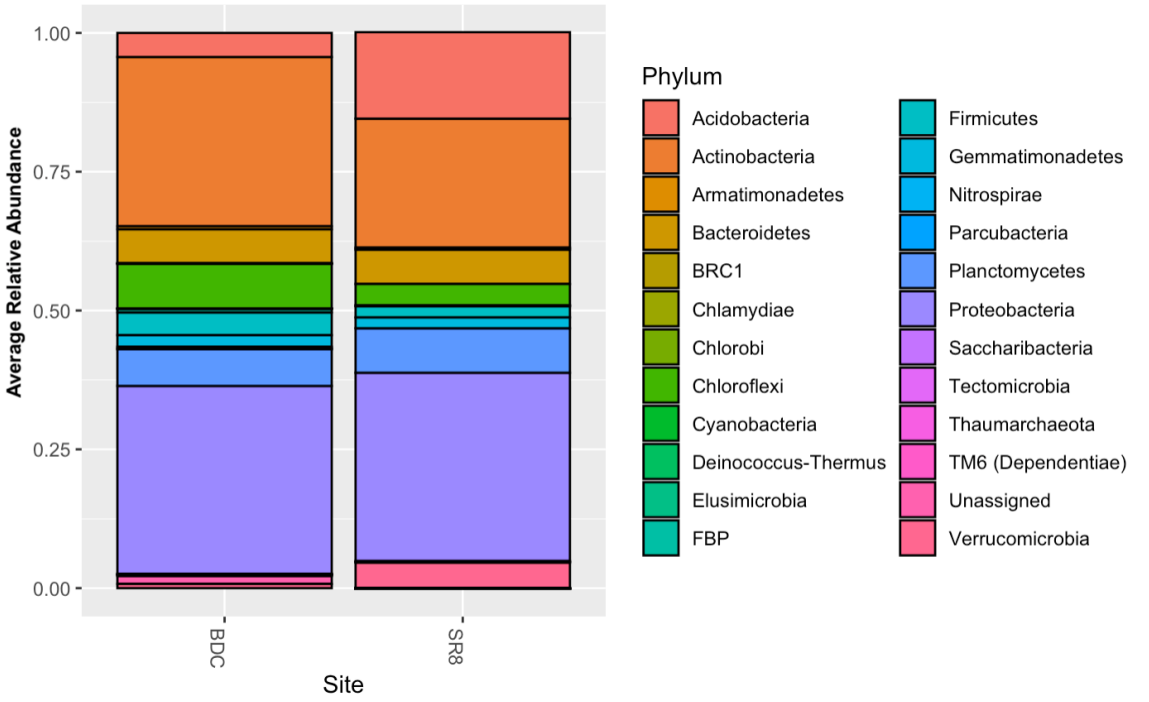

Figure 1.7: Comparison of Bacterial Phyla: The average relative abundance of bacterial phyla in pretreatment soils at the desert site Boyd Deep Canyon (BDC) and the forest site Santa Rosa Peak (SR8).

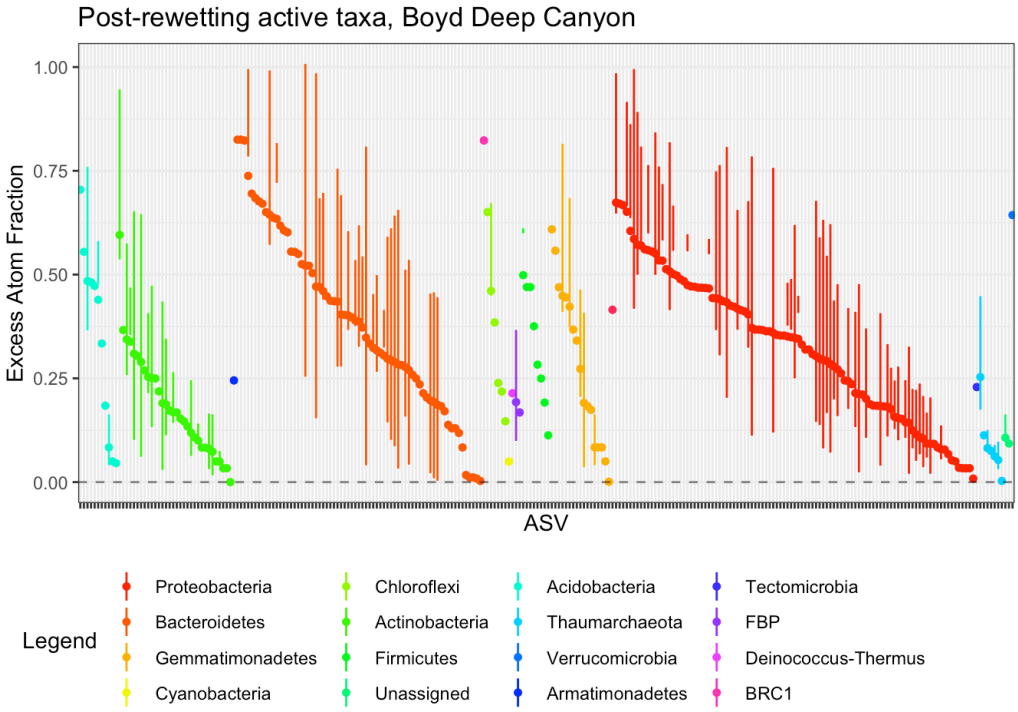

Figure 1.8: Desert bacterial taxa active post-rewetting: Each point represents an ASV. Errorbars represent the 95% confidence intervals of mean excess atom fraction (EAF) determined with bootstrapping. Color represents the phylum and each phylum is sorted from high to low EAF. All taxa shown below have a lower confidence interval > 0 and are therefore considered to be incorporators of $H_2{}^{18}O$. Incorporation of $H_2{}^{18}O$ following rewetting indicates that the taxa had significant amounts of biomass growth following rewetting.

Supplementary Table 1.1: qSIP calculations

Excess Atom Fraction Calculation		
Step	Equation	Explanation
1	$y_{ijk} = P_{ijk} + f_{jk}$	The total number of 16S copies of a single taxon i in a single fraction *k* in replicate *j* (y_{ijk}) is calculated as the proportional abundance of *i* within *k* (determined by sequencing) times the total copies of 16S gene copies in that fraction (determined through qPCR).
2	$Y_{ij} = \sum_k [y_{ijk}]$	The sum of the total number of genes copies of taxon *i* across all *k* fractions in replicate *j*
3	$W_{ij} = \sum_k [x_{jk} * (y_{ijk} / y_{ij})]$	The total density of taxon *i* across all *k* fractions of replicate *j* (W_{ij}) is the sum of proportional densities, calculated by multiplying the density x in each fraction by the proportional gene copies in each fraction (y_{ijk} / y_{ij})
4	$Z_i = W_{lab(i)} - W_{light(i)}$	The change in density caused by ^{18}O isotope incorporation is calculated for each taxon *i* as the difference between the mean W_{ij} for all *j* replicates from the ^{15}N ($W_{lab(i)}$) and ^{14}N ($W_{light(i)}$) treatments
5	$G_i = (1 / 0.083596) * (W_{lighti} - 1.646057)$	The GC content of taxa *i* is calculated from the mean density from the ^{16}O treatments.
6	$M_{lighti} = 0.496 * G_i + 307.691$	The GC content is then used to calculate the natural (e.g. incubated with ^{16}O) molecular weight of taxa *i*'s DNA sequence
7	$M_{heavymaxi} = 12.07747 + M_{lighti}$	The theoretical maximum molecular weight of taxa i's DNA sequence (i.e. if every oxygen atom in newly synthesized DNA was ^{18}O) is calculated from the natural abundance molecular weight.
8	$M_{labi} = (z_i / W_{lighti} - 1) * M_{lighti}$	The molecular weight of DNA for taxon *i* in the labeled treatment (M_{labi}) was calculated from the proportional increase in density (*Zi)* relative to the density of the unlabeled treatments (W_{lighti})
9	$A_{oxygeni} = (M_{labi} - M_{lighti}) / (M_{heavymaxi} - M_{lighti}) * (1 - 0.002000429)$	The proportional change in molecular weight of taxa i's 16S DNA sequence due to isotope incorporation, $A_{oxygeni}$, aka excess atom fraction, was calculated accounting for the background fractional abundance of ^{18}O.

Supplementary Table 2: Dothideomycetes of Boyd Canyon

Genus	**Species present**	**Response to N addition**	**Potential Function**
Alternaria	*A. chlamydosporigena* *A. subcucurbitae*	-	Plant Pathogen
Ascochyta	*A. pisi*	NA	Plant Pathogen
Aureobasidium	*A. melanogenum*	NA	Black yeast
Coniothyrium	*C. palmicola* *C. telephii*	+	Endophyte
Deniquelata	*D. barringtoniae*	+	Plant Pathogen
Dictyosporium	*D. heptasporum*	NA	Saprotroph
Didymella	*D. glomerata*	NA	Plant Pathogen
Hormonema	*H. viticola*	NA	Black yeast
Kalmusia	Unassigned	NA	NA
Phoma	Unassigned	NA	NA
Pleiochaeta	*P. carotae* *P. setosa*	+	Plant Pathogen
Preussia	*P. africana* *P. fleischhakii* *P. terricola*	-	Endophyte, Plant Pathogen

Supplementary Figure 1: Alpha Diversity

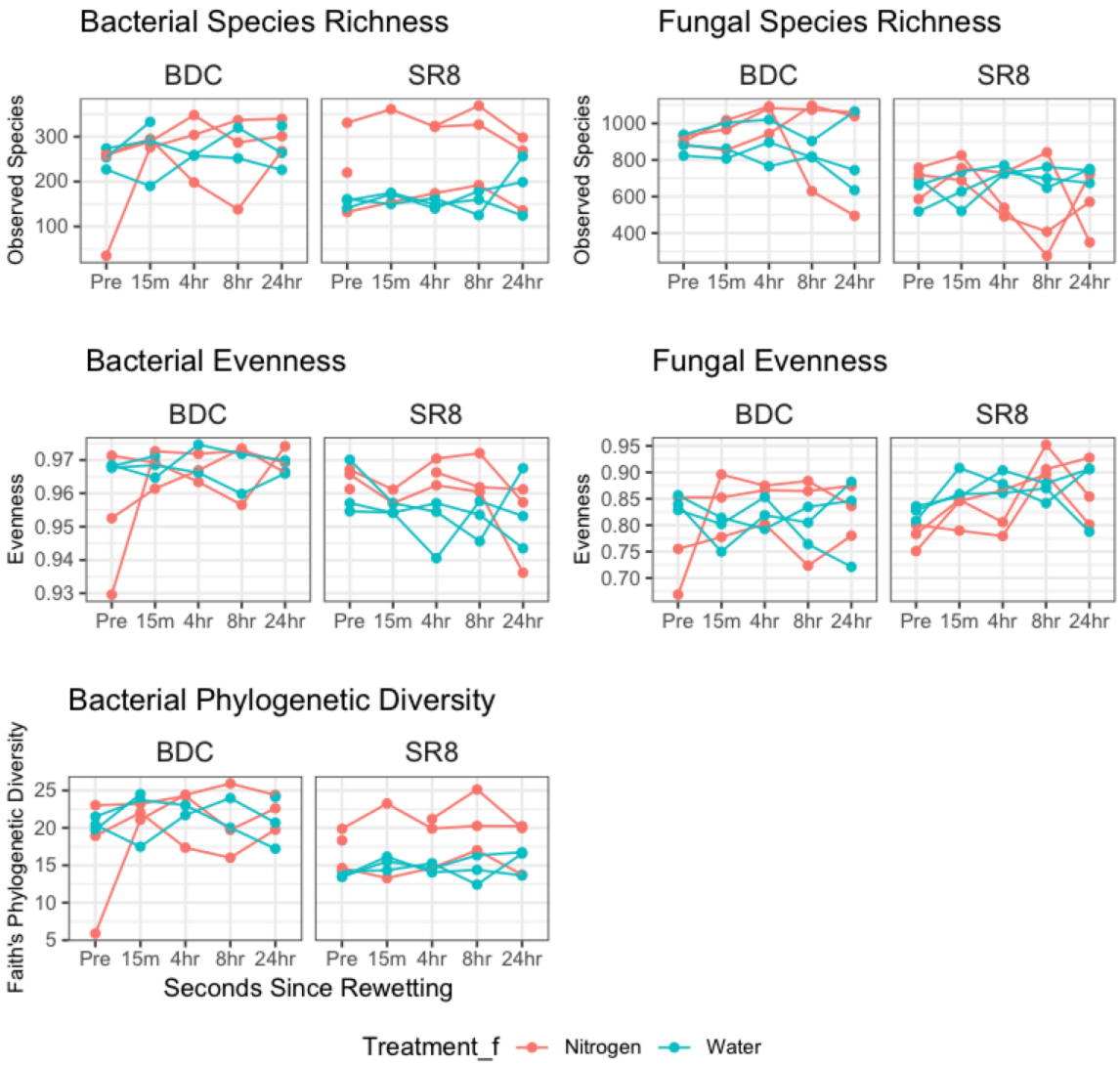

Supplementary Figure 1.2: Relative abundance of Dothideomycetes over time and in response to nitrogen at Boyd Deep Canyon

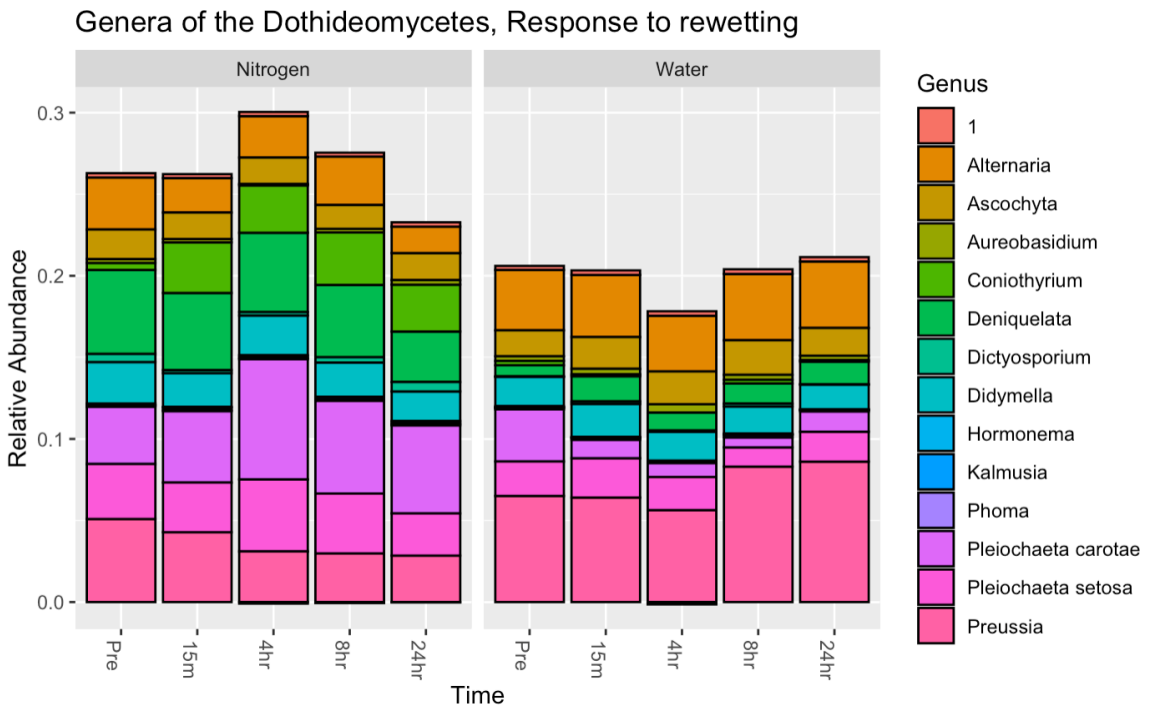

Supplementary Figure 3: Putative N emitting bacteria

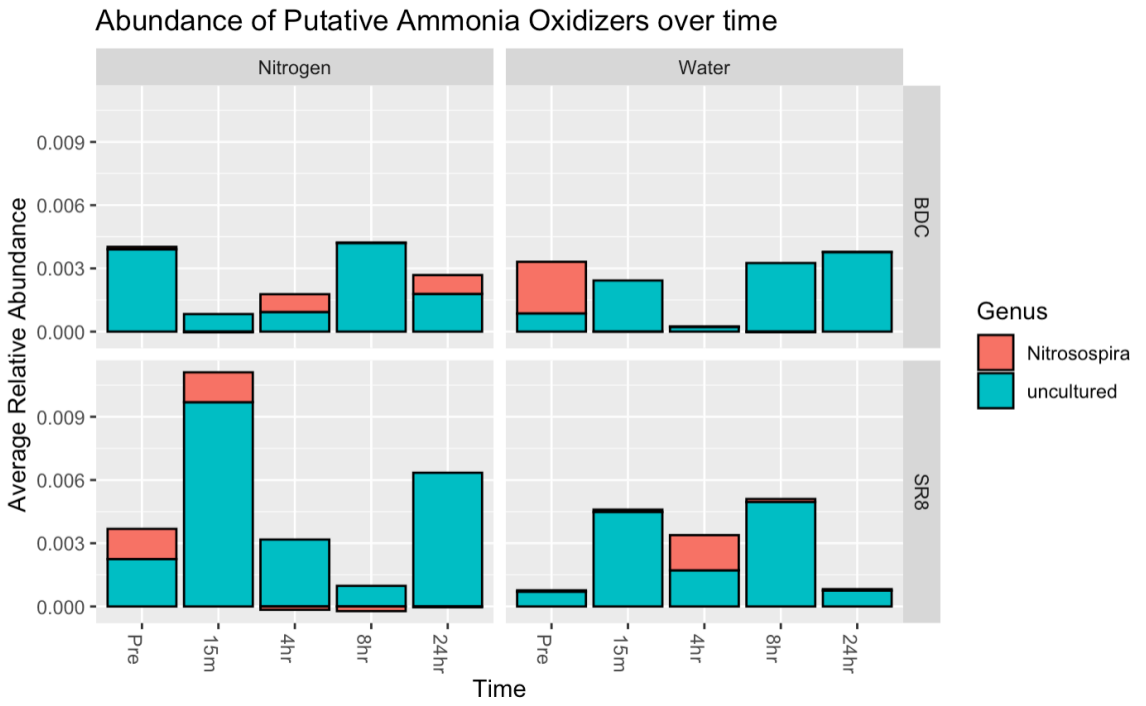

Chapter 2: Bacterial assimilation of ammonium across an atmospheric nitrogen deposition gradient

Introduction

Nitrogen deposition alters soil biogeochemistry through the soil microbiome. Studies on the effects of nitrogen deposition on soil microbial dynamics in other multiple ecosystems point to a relationship between available mineral nitrogen (N), soil carbon (C), and microbial composition that increases bacterial metabolism and emissions of N and C: For example, in forest systems N-dep decreases soil carbon stocks by increasing AM over EM fungi, as EM are thought to stabilize soil C by limiting decomposer access to N and decreasing microbial respiration (Averill et al., 2018). This favoring of bacterial decomposer processes was also seen reflected in the functional gene composition of forest bacteria, as N-dep in forests has also been found to increase bacterial carbohydrate metabolism (Freedman et al., 2016). Even moderate loads of N-dep in forests may change the fungal community but not the bacterial community (Frey et al., 2020), indicating that soil fungi are more sensitive to N-dep.

While desert and forest soils are different in a multitude of ways, this mechanism of N-dep favoring soil bacterial processes may be similar. N-dep changes plant-soil microbial interactions by altering the composition of soil bacteria (He et al., 2022; Z. Wang et al., 2020). The dominant soil clades Proteobacteria, Acidobacteria, and Actinobacteria were found to be specifically sensitive to N-dep (Jia et al., 2021). N-dep dynamics in deserts and other arid systems are likely to be particularly important during the large pulses of microbial activity and soil respiration following rewetting of dry soils.

In this context, high concentrations of solubilized mineral N likely overwhelm microbial N demand, with the effect on pH and soil matric potential, creating elevated nitrification and N loss from the system.

Microbes transform mineral nitrogen into biomass during biogeochemical pulses. A significant amount of biogeochemical activity occurs in the hours to days following rewetting of dry soils in arid ecosystems. Nitrogen is lost from the soil as NO_x and N_2O gases from a complex interaction of biotic microbial transformations and abiotic reactions of N intermediates with the soil matrix. In chapter 1 and again in chapter 3, I focus on the competing and co-occurring microbial processes that result in N gas emissions, such as fungal and bacterial denitrification. In this chapter, however, I will focus on a different route for soil nitrogen: sequestration into microbial biomass. The observed relationships between N emissions and soil carbon points to biomass building processes being a competing sink for N: The amount of N lost from the system is influenced by soil C levels, as higher amounts of available C increase the amount of respiration in response to added N (Eberwein et al., 2015) and results in more of the N pulse assimilated into microbial biomass (Schaeffer et al., 2003; Fierer & Schimel, 2002; Zhang et al., 2018). The assimilation of N into organic molecules (i.e. nitrogen immobilization) can therefore be seen reciprocal process to N emissions, with the potential to mitigate the loss of N as NO_x and N_2O emissions.

It is understood that heterotrophic organisms prefer NH_4 as a source of N for biomass building, which represents the final nitrogenous product of organic matter decomposition, and is taken up by microbes via the mineralization-immobilization-transformation (MIT) route (Geisseler et al., 2010). However, the soil microbes capable of assimilating N into microbial biomass and what edaphic traits influence this process is

unclear. For example, while NH_4 is a universal source of assimilatory nitrogen with virtually all prokaryotes possessing the necessary genes, it has been shown that in soils, greater than 80% of active nitrogen assimilation is performed by only a small group of bacterial orders (Morrissey et al., 2018). In arid grasslands, total rates of microbial growth post rewetting peaks within 24 hours, but the diversity of growing microbes steadily accumulates over time and peaks 7 days post rewetting (Blazewicz et al., 2020). This effect of rewetting on diversity is thought to be a combination of copiotrophic fast responding microbes able to rapidly detect available C and N, and oligotrophic bacteria that need longer to initiate growth.

Therefore, the aim of this experiment is to determine how atmospheric nitrogen deposition impacts the soil bacterial community capable of assimilating NH_4 into bacterial biomass during a rewetting pulse. For this study, I used soils taken from across a nitrogen deposition gradient in southern California to analyze assimilation of N across with increasing levels of N-dep. Analysis of bacterial communities by 16S marker gene sequencing will be combined with quantitative stable isotope probing (qSIP) in order to analyze patterns of bacteria diversity before and after rewetting, which taxa are able to grow on the provided nitrogen source following rewetting, and the relative amounts of nitrogen turnover occurring across bacterial clades. My hypotheses for this experiment are:

1. Nitrogen deposition will alter the composition of the soil microbiome by decreasing diversity of the total soil bacteria but increasing the diversity of mineral N incorporators. Previous studies have shown that N-dep decreases diversity of bacteria while also reducing fungal activity, diversity, and soil carbon

levels (T. ’an Zhang et al., 2018). I suspect that this is due to the selection for copiotrophic bacterial metabolism, which is less reliant on the products of saprotrophic decomposition and the presence of complex organic matter. If copiotrophs are selected for by N-dep, there should be a higher number of and phylogenetic diversity of bacteria capable of incorporating mineral N in the form of NH_4.

2. There will be an increase in total nitrogen sequestered as bacterial biomass across the nitrogen deposition gradient due to the increased abundance of specific bacterial clades.

Methods

Study Sites: Soils were sampled from three dryland sites in Southern California: Pinto Basin, Wide Canyon, and Morongo Canyon. These three sites fall along a transect stretching from the edge of Joshua Tree National Park to the source of N-dep: an urban thermal plume originating in the Los Angeles metropolitan area. This transect therefore covers a gradient of increasing nitrogen deposition. Pinto Basin receives an average of 4.3 Kg N ha^{-1} yr^{-1} and has a pH of 8.17 ∓ 0.36. Wide Canyon receives an average of 6.4 Kg N ha^{-1} $yr^{-1,}$ and has a pH of 8.17 ∓ 0.36. Morongo Canyon receives and average of 15 Kg N ha^{-1} yr^{-1} and has a pH of 6.78 ∓ 0.32. Pinto Basin and Wide Canyon have been described extensively in (Rao et al., 2009; Rao & Allen, 2010). All soils were either loamy sand or sandy loam and dominated by creosote bush, *Larrea tridentata.* I sampled soils in July 2019 at the end of the summer dry season, when all sites had no rainfall in the 30 days prior to sampling.

Soil collection, nitrogen incubations, and DNA extraction: One soil sample was collected at a depth of 5cm from underneath the canopy of 4 individual creosote shrubs at each site (n=4). Soils were then subsampled for soil chemical analysis, nitrogen incubations, and DNA extraction as described below. All analyses methods were performed on dry soils and soil incubated for 7 days.

For soil chemical analyses, 50g of dry soil was incubated in sealed jars with 16.6 mL of water alone or a solution of NH_4 Cl (final concentration 126.3 ug per g dry soil). Gravimetric water content was determined for 10g of soil at 105°C. Nitrogen was extracted from 5g of soil by shaking in 30mL 2 M KCl (30 mL) for one hour. Solutions were then filtered using 2.5 µm filter paper and frozen until analysis. Colorimetric assays

were performed at the Environmental Sciences Research Laboratory at the University of California, Riverside to measure soil extractable NH_4 (SEAL method EPA-126-A), NO_3 (SEAL method EPA-129-A). To determine microbial biomass nitrogen and carbon, I used simultaneous chloroform fumigation-extraction (Fierer, 2003). Briefly, 5 g of each soil was incubated with 40 mL of 0.5M K_2SO_4 alone or with additional 0.5 mL chloroform at 150 rev min^{-1}. Incubation solutions were then filtered through Whatman No. 1 paper and bubbled with air for 20 m. Extracts were analyzed at the UCR-ESRL for dissolved C and N using the persulfate digestion technique. Extractable microbial biomass N and C is then calculated as the difference between the chloroform exposed and control samples for each soil and corrected assuming 40% of microbial biomass was extracted (Dictor et al., 1998).

To incubate soils for stable isotope probing, three grams of soil were added to 15-mL Falcon tubes with treatments of either $^{15}NH_4Cl$ (atom fraction 97%, final concentration of 128.6 ug per g dry soil) or NH_4Cl (final concentration 126.3 ug per g dry soil) in 1 mL H_2O. Time 0 samples received no water and were immediately frozen at -80°C until further processing. Samples with added nitrogen were incubated for 7 days (168 hours) and then stored at -80°C until further processing. DNA was extracted in triplicate (total = 0.9g soil) from each sample using PowerLyzer PowerSoil DNA Isolation Kit according to the manufacturer's instructions, with an initial 25-min incubation at 65°C. DNA was quantified with a Qubit Fluorometer (LifeTechnologies, Carlsbad, California, USA).

CsCl density gradient centrifugation and fractionation: To separate DNA by density, 3.5 ug of DNA from each sample was added to approximately 3mL of a saturated CsCl and gradient buffer solution in a 3.3-mL OptiSeal ultracen-trifuge tube

(Beckman Coulter, Fullerton, California, USA). The samples were spun in an OptimaMax benchtop ultracentrifuge (Beckman Coulter) using a Beckman TLN-100 rotor at 127,000 x g for 72 h at 18°C. After centrifugation, each density gradient was divided into 24 fractions of 40 uL. The density of each fraction was measured and DNA was then purified from the CsCl solution using isopropanol precipitation and resuspended in 50uL sterile deionized water. The fractions within the density range of 1.6800-1.7600 g/mL were used to move forward with qPCR and sequencing. There were a total of 9 fractions per sample within this range, with fractions between 1.7050-1.6800 were merged together into a single sample.

Quantitative PCR: I used qPCR to determine copies of the 16S rRNA gene in each density fraction. Standard curves were generated using 5-fold serial dilutions of the ZymoBIOMICS Microbial Community Standard. Triplicate 10 uL reactions included: 1 uL of template DNA, 0.25 uM of each primer (388F, 5'-GCTGCCTCCCGTAGGAG-3' and 518R 5'-ATTACCGCGGCTGCTGG-3',), Forget-Me-Not EvaGreen qPCR Master Mix (Biotium), and 1.5mM $MgCl_2$. Reactions were performed on a CFX384 Touch Real-Time PCR Detection System (Bio-Rad Laboratories) using a program of 95°C for 2 min followed by 40 cycles of 95°C for 30 s, 64.5°C for 15 s, and 72°C for 15 s. All reactions had an efficiency > 85% and R^2 > 0.9990. Based on qPCR data, two samples (one ^{15}N incubation from Wide Canyon and one ^{14}N control incubation from Morongo Canyon) were excluded from downstream analysis due to insufficient DNA quantities.

16S rRNA gene sequencing: High-throughput sequencing of the 16S rRNA gene was performed on individual density fractions for all samples. The V4 region of the 16S rRNA gene was amplified using the 515F (5'-GTGCCAGCMGCCGCGGTAA-3') and 806R (5'-GGACTACVSGGGTATCTAAT-3') primer set. DNA was amplified using

Phusion Hot Start II Polymerase (Thermo Fisher Scientific, Waltham, Massachusetts,USA), Phusion HF buffer (Thermo Fisher Scientific), 1.5 mM $MgCl_2$ and 0.25 µM of each primer. The reaction was carried out with the following thermocycle: Initial denaturing at 95°C for 3 minutes, followed by 30 cycles of 95°C for 30 seconds, 55°C for 30 seconds, 72°C for 30 seconds, and concluding with a final extension at 72°C for 5 minutes. Initial PCR products were used as template in the indexing reaction (10 cycles identical to initial amplification conditions) to add barcodes and Illumina flowcell adapter sequences. The Indexed PCR products were purified with carboxylated Sera-Mag SpeedBeads (Sigma-Aldrich, St. Louis,Missouri, USA) at a 1:0.8 v/v ratio and quantified by QuBit fluorescence. Equal volumes of the reaction products were then pooled into the final library. The library was then submitted to the University of California, Riverside Genomics Facility to be sequenced with paired ended 300bp reads on the Illumina MiSeq platform.

Sequence processing and bioinformatics: Demultiplexed 16S sequences were analyzed in QIIME2 (Bolyen et al. 2019). Reads were trimmed to 230 base pairs and DADA2 was then used to remove chimeras, quality filter, and pick amplicons sequence variants (ASVs). ASV sequences were assigned taxonomy with a bayesian classifier using reference sequences from the SILVA database release 132 (Quast et al. 2013). Data from a negative sequencing control was used to remove <20 contaminant OTUs. Singletons, doubletons, and ASVs that made up <0.005% of total read abundance were removed for all analyses. After processing and filtering, there were a total of 2,820,550 16S reads classified into 4,222 ASVs.

Estimating excess atom fraction and nitrogen flux: Excess atom fraction caused by incorporation of the 18O was then calculated following the protocol outlined in

(Hungate et al., 2015; Morrissey et al., 2018) and summarized in Chapter 1. Growth rates and amount of nitrogen assimilated into microbial biomass were calculated based on (B. J. Koch et al., 2018) and summarized in Supplementary Table 1. Adjustments for using ^{15}N instead of ^{18}O are made to the following equations from supplementary table 1.1:

Step 7: $M_{heavymax_i} = 0.5024851*Gi + 3.5173961 + M_{light_i}$

Step 9: $A_{oxygen_i} = (M_{lab_i}-M_{light_i}) / (M_{heavymax_i}-M_{light_i}) * (1-0.003663004)$

Diversity analysis of total and incorporator taxa: ASV data was processed in different ways depending on how the data was analyzed. For the analyses performed on total observed taxa (i.e. including non-incorporator taxa), only natural abundance N and pretreatment controls were used. To analyze beta diversity across sites for all observed taxa, data were normalized using centered log-ratio (clr) transformation in the R package ANCOMBC (Lin & Peddada, 2020b). Community composition was analyzed by PCoA of an aitchison distance matrix using the Phyloseq package in R (McMurdie & Holmes, 2013). To analyze alpha diversity for all observed taxa, data was normalized to relative abundance and then used to calculate richness, evenness, and faith's phylogenetic diversity. Beta and alpha diversity analyses were performed on incorporator taxa using their EAF values.

Results

Composition of total observed taxa: I analyzed 16S data from the natural abundance N (^{14}N) and pretreatment samples to determine alpha and beta diversity patterns across the N-dep gradient. Overall, site was the largest driver of bacterial composition and there were significant changes in composition across time [PERMANOVA site: F=8.25, p=0.002; hour: F= 4.74, p=0.002]. However, principal coordinate analysis shows that while fractions cluster by site, Pinto Basin clusters closer to Morongo Canyon than Wide Canyon despite N dep, pH, and geographical patterns (Fig. 2.1). Post-rewetting, there is a shift in composition such that Morongo and Wide Canyon are more alike and clustering pattern more closely mimics geographical/N-dep pattern, however there was not a larger effect of site on composition before or after rewetting. The magnitude of compositional changes were different across sites [PERMANOVA F=2.20, p=0.002] with less community turnover in response to rewetting event and N addition with increasing exposure to nitrogen deposition (Supplementary Fig. 2.1).

Diversity of total observed taxa: Pre-rewetting**,** N-dep was not the primary driver of pre-wetting total species richness, as there were a similar number of total observed species at all three sites, and the highest mean species at Wide Canyon (Fig. 2.2). However, all sites had increased richness after incubation [ANOVA F=12.131, p=0.008]. There were approximately 400 total observed bacteria ASVs in all dry soils and 500-600 in rewet soils (Fig. 2.2). However, site did significantly affect the phylogenetic diversity of soil bacteria [ANOVA F=35.91, p=1e-3]. Higher nitrogen deposition soils had more phylogenetically diverse bacteria communities in dry soils and larger increases in bacterial diversity post-rewetting (Fig. 2.2) [ANOVA F=7.66,p=0.01].

Across all sites, about 38% of taxa found 7 days post rewetting were not found pre-rewetting, indicating that the biomass of these taxa were too low at time 0 to be captured with sequencing.

NH_4 incorporators: The mean density change of 16S rDNA in the ^{15}N incubations compared to the control natural abundance N incubations change was above zero at all sites, indicating sufficient isotope incorporation to estimate excess atom fraction values for this experiment. The mean density change was different across sites (ANOVA F = 9.372, p = 1e-4), with higher mean increase in density at Pinto Basin (0.0017189) and Wide Canyon (0.001729) compared to Morongo Canyon (0.0002556).

There were 100-150 incorporating taxa in each shrub at each site, and there was no effect of site on the richness of incorporator taxa (Fig. 2.2). Similar to the pattern seen for total observed bacteria species, the phylogenetic diversity of incorporators was different across sites [ANOVA F=20.09, p=0.001], with higher diversity in the two higher N-dep sites: Wide Canyon and Morongo Canyon (Fig. 2.2). At all four sites, the majority of incorporators were from 9 phyla: Proteobacteria, Actinobacteria, Acidobacteria, Bacteroidetes, Firmicutes, FBP, Chloroflexi, Gemmatimonadetes, and the Thaumarchaeota (Fig. 2.3). Each of these phyla had at least 10 incorporators and made up > 1% of total incorporators. There were 30 orders of incorporators within these Phyla (Table 2.1). Across all sites, the 4 major incorporator orders were Rhizobiales, Burkholderiales, Frankiales, and Sphingomonadales. The ASVs belonging to these orders made up 5-18% of total incorporator taxa at each site. As nitrogen deposition increased, the number of Rhizobiales incorporators decreased from 68 (18%) to 20 (6%). Incorporators from the order Blastocatellales increased with nitrogen deposition from 6 (1.6%) to 44 (13.79%).

Soil chemistry: Before rewetting, site is a driver of microbial biomass nitrogen (MBN) [ANOVA F=10.44, p=0.004], and extractable NO_3 [ANOVA F=20.8, p=0.0004], both increasing with N deposition (Fig. 2.4). However, there was no effect of site on microbial biomass carbon (MBC) or extractable NH_4 in dry soils. Added NH_4 increased extractable NH_4 after 7 days by an average of 22 ug per g soil at all sites. When incubated with H_2O alone, there were not significant increases in MBC or MBN. However, NH_4 treatment changed MBN compared to the water only control (ANOVA F=27.51, p=0.0005], but not MBC.

Estimated nitrogen assimilation: Based on the growth model from (Koch et al., 2018), I estimated the amount of nitrogen assimilated as microbial biomass for each ASV. There was not a significant difference in total ENA across sites or a significant relationship between ENA and phylogenetic diversity or species richness. However, analysis of ENA for individual orders shows that N-dep might be altering order level assimilation of nitrogen by altering microbial biomass: The amount of microbial biomass in the soil before rewetting was significantly correlated to the ENA of Cytophagales [ANOVA F=15.62, p=0.0042] and Blastocatellales [ANOVA F=6.2,p=0.03], and as stated above, was significantly higher with increasing nitrogen deposition.

Discussion & Conclusions

These results confirm previous studies that have indicated that despite capacity for NH_4 assimilation being a broadly distributed trait, in actively metabolizing soils the majority of bacterial nitrogen assimilation is carried out by a handful of key orders (Morrissey et al., 2018). My first hypothesis, that nitrogen deposition would increase the diversity of NH_4 assimilators while decreasing total observed bacteria, is partially supported by these results. There was a higher phylogenetic diversity of assimilators in higher N-dep soils, but N-dep did not affect the diversity of total observed bacteria.

On the global scale nitrogen deposition is known to reduce soil microbial diversity, but these results show that at the regional scale, N-dep was not the primary driver of total bacterial diversity, which did not significantly change across the nitrogen deposition gradient. These data suggest that N-dep interacts with other soil properties to influence the soil microbiome: In my analysis of the effect of N-dep on dry soils produced by the long dry-down period that sets the stage for the rewetting processes, I found that Wide Canyon, the middle site in the gradient, had the highest species richness. This is likely due to the effects of pH, as Wide Canyon has a pH of 7.28 and bacterial populations are more diverse when approaching soil pH (Lauber et al., 2009). Wide Canyon also had the highest bacterial species richness after rewetting, and the greatest increase in total microbial biomass in response to NH_4 treatment.

It is difficult to parse the influence of pH and N-dep in this study system as the processes affecting rainfall and annual nitrogen load are intertwined. However, these results show that despite the diversity pattern seen in dry soils, after rewetting with the N tracer, SIP analysis shows that increasing N-dep produces a higher phylogenetic diversity of N-assimilating microbes, specifically increasing the number of N-assimilating

bacterial families within the Proteobacterial and Actinobacterial Phyla. However, despite having a more diverse pool of assimilators, as N-dep increased there was no increase in microbial biomass, and total community turnover was decreased.

In these soils, one of the most significant families that increased in abundance and assimilation across the N-dep gradient was the Sphingomonadales. This family has been shown to be responsible for the expression of stress-associated genes in disturbed rhizospheres, including fungicidal enzymes (Chapelle et al., 2016). Increased abundance of Sphingomonads is also seen in highly fatigued agricultural soils (Wolińska et al., 2018). Therefore, the increasing richness of sphingomonad incorporators with increasing nitrogen deposition could be related to an ability to grow on mineral N or their competitive interactions with soil fungi, which other studies have shown are decreased by N-dep.

In conclusion, these results show that in desert soils, nitrogen deposition increases diversity of N-assimilators but not microbial biomass post rewetting. Although increased biodiversity is typically thought to have more beneficial effects on ecosystem processes, in this case increased N-assimilators is likely part of a more complex network of effects of N-dep, including the selection of bacterial over fungal metabolism in a way that increases N losses from the system. Further research is needed to examine the functional traits of these bacteria up-regulated by N-dep in order to gain a better mechanistic understanding of how bacterial metabolism affects the fate of soil nitrogen stocks.

Figures & Tables

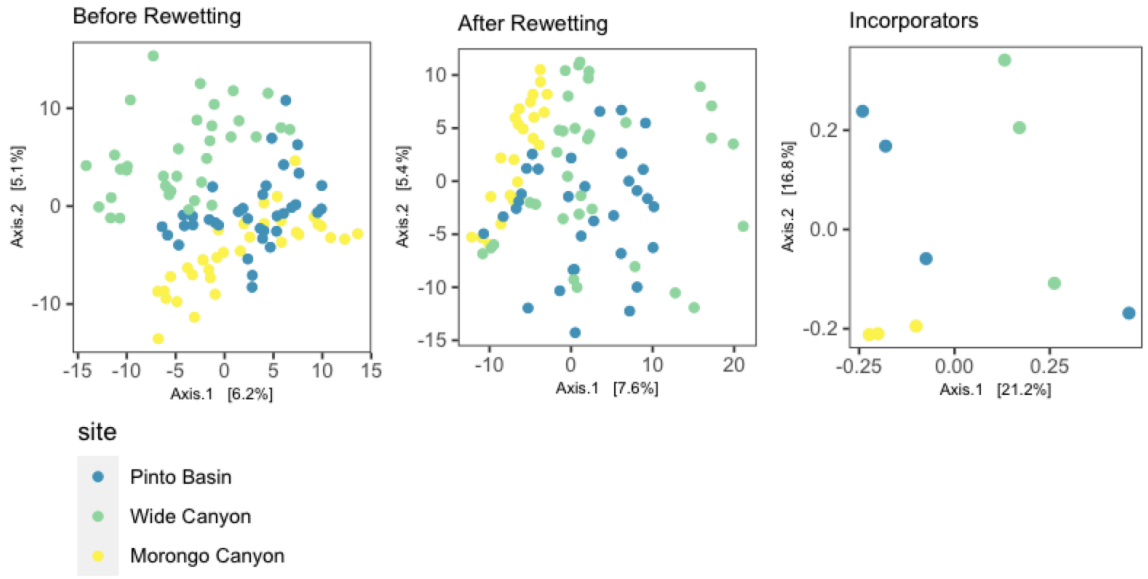

Figure 2.1: Bacterial composition before and after rewetting. PCA of aitchison distances. Each point represents a fraction of DNA extract. Left panel shows dry soils before rewetting (t0), middle panel 7 days/168 hours post NH_4 incubation (t168). The right panel shows ordination by EAF values. Color represents site: Pinto Basin (low N-dep), Wide Canyon (moderate N-dep) and Morongo Canyon (high N-dep).

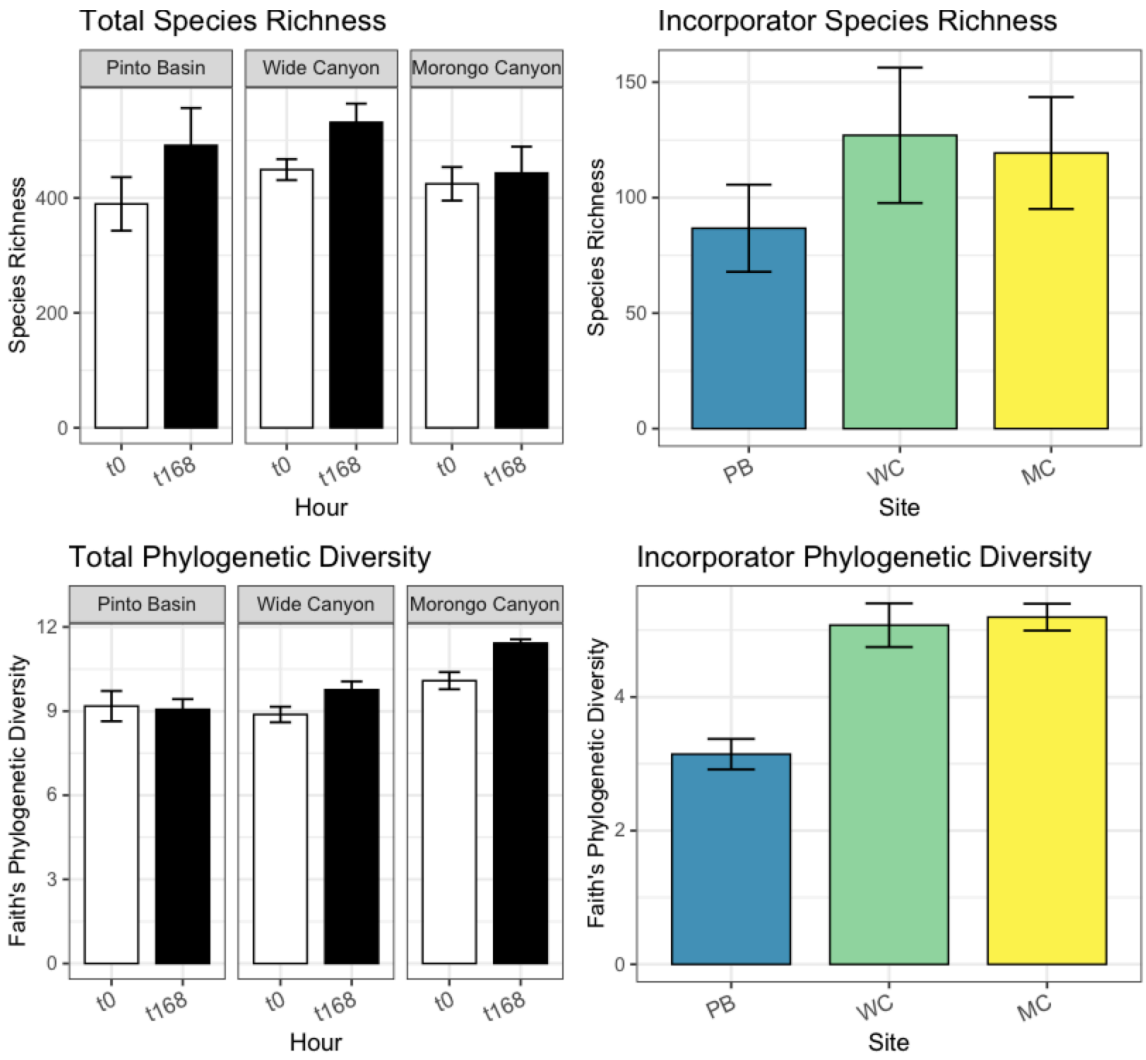

Figure 2.2: Alpha Diversity. Two measures of alpha diversity - species richness and phylogenetic diversity (faith's pd) were calculated before rewetting (t0) and 7 days/168 hours post rewetting (t168).

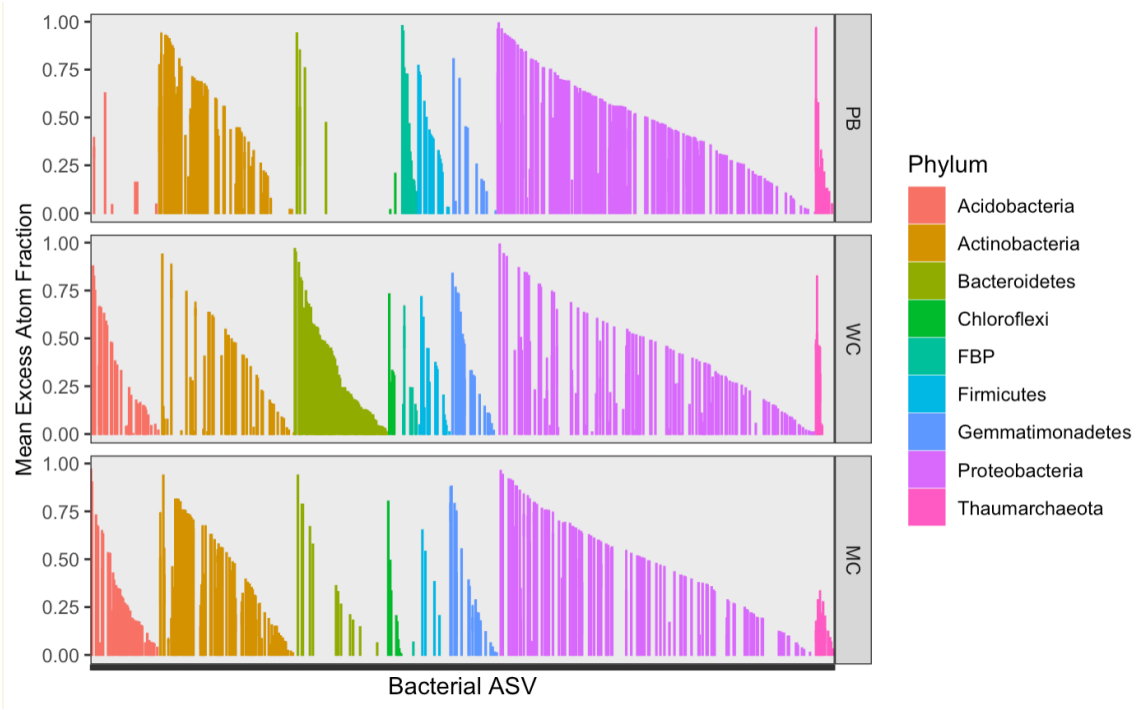

Figure 2.3: Phylum level N-assimilators Across N-dep Gradient: Each line represents the mean EAF of a bacterial ASV capable of assimilating NH_4. Color represents Phylum.

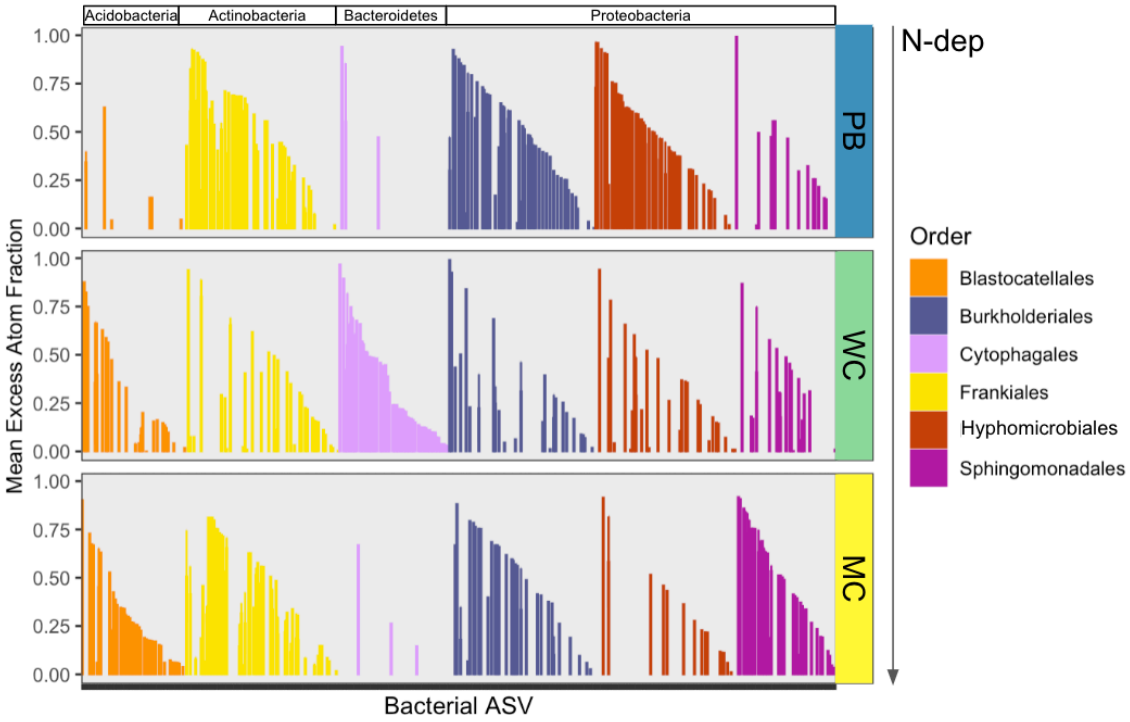

Figure 2.4: Key Order-level N-assimilators Across N-dep Gradient: Each line represents the mean EAF of a bacterial ASV capable of assimilating NH_4. Color represents Order.

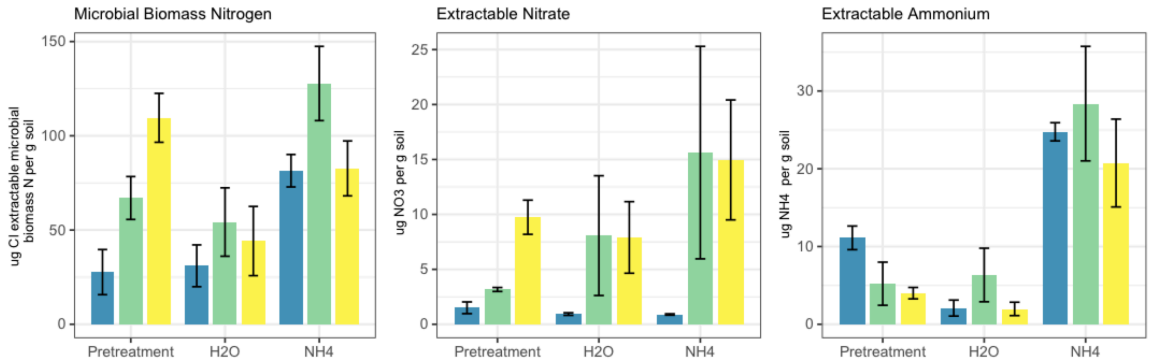

Figure 2.5: Impact of nitrogen treatments on soil nitrogen dynamics.

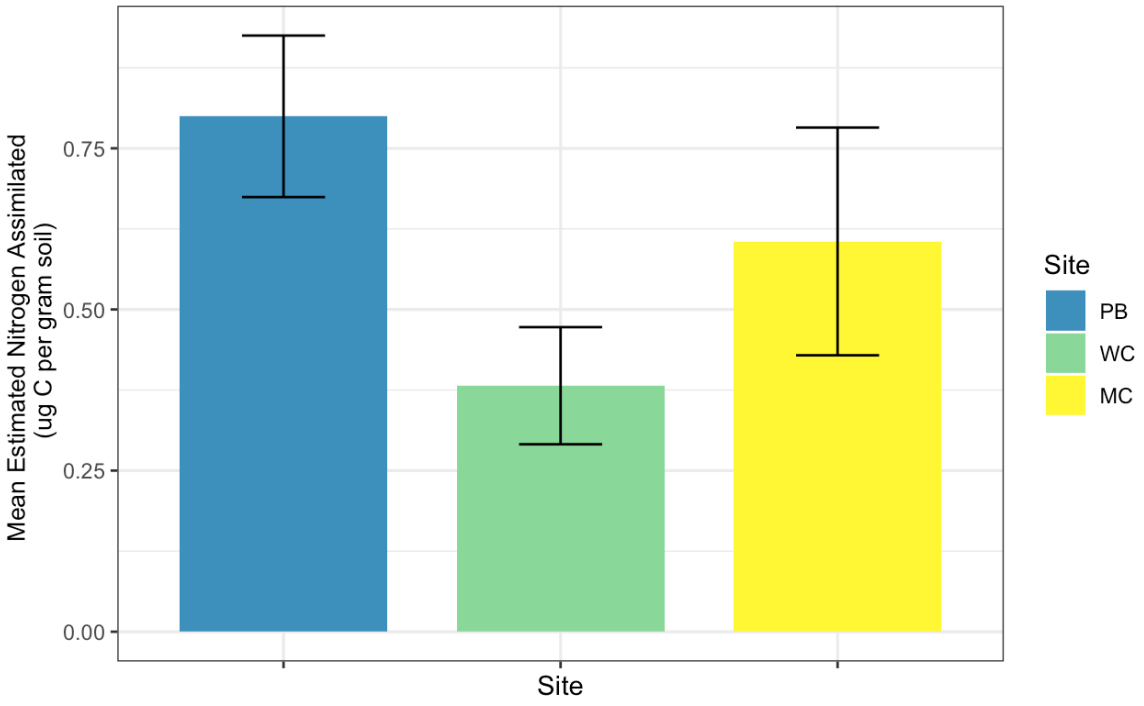

Figure 2.6: Mean Estimated Nitrogen Assimilated Across the N-dep Gradient

Table 2.1: Orders of NH_4 incorporating bacteria: Summary of the richness (#) and percentage of incorporators for each bacterial order at each site.

Pinto Basin		Wide Canyon		Morongo Canyon			
#	%	#	%%	#	%	Order	Phylum
68	18.18%	31	8.73%	20	6.27%	Rhizobiales	Proteobacteria (alpha)
61	16.31%	30	8.45%	39	12.23%	Burkholderiales	Proteobacteria (beta)
58	15.51%	40	11.27%	49	15.36%	Frankiales	Actinobacteria
21	5.61%	21	5.92%	41	12.85%	Sphingomonadales	Proteobacteria (alpha)
15	4.01%	5	1.41%	3	0.94%	Rhodobacterales	Proteobacteria (alpha)
14	3.74%	12	3.38%	7	2.19%	Rhodospirillales	Proteobacteria (alpha)
13	3.48%	5	1.41%	9	2.82%	Micromonosporales	Actinobacteria
12	3.21%	11	3.10%	0	0.00%	Clostridiales	Firmicutes
10	2.67%	4	1.13%	4	1.25%	Bacillales	Firmicutes
8	2.14%	11	3.10%	8	2.51%	Myxococcales	Proteobacteria (delta)
8	2.14%	0	0.00%	0	0.00%	Pseudomonadales	Proteobacteria (gamma)
7	1.87%	15	4.23%	14	4.39%	Gemmatimonadales	Gemmatimonadetes
6	1.60%	24	6.76%	44	13.79%	Blastocatellales	Acidobacteria
6	1.60%	7	1.97%	3	0.94%	Longimicrobiales	Gemmatimonadetes
6	1.60%	0	0.00%	8	2.51%	Caulobacterales	Proteobacteria (alpha)
5	1.34%	7	1.97%	3	0.94%	Micrococcales	Actinobacteria
5	1.34%	0	0.00%	1	0.31%	Xanthomonadales	Proteobacteria (gamma)
4	1.07%	56	15.77%	3	0.94%	Cytophagales	Bacteroidetes
4	1.07%	1	0.28%	4	1.25%	JG30-KF-CM45	Chloroflexi
3	0.80%	20	5.63%	1	0.31%	Nitrosomonadales	Proteobacteria (beta)
2	0.53%	7	1.97%	3	0.94%	Solibacterales	Acidobacteria
2	0.53%	0	0.00%	6	1.88%	Solirubrobacterales	Actinobacteria
2	0.53%	1	0.28%	8	2.51%	Pseudonocardiales	Actinobacteria
1	0.27%	0	0.00%	0	0.00%	Subgroup 10	Acidobacteria
1	0.27%	24	6.76%	10	3.13%	Sphingobacteriales	Bacteroidetes

0	0.00%	3	0.85%	1	0.31%	Subgroup 7	Acidobacteria
0	0.00%	0	0.00%	4	1.25%	Streptomycetales	Actinobacteria
0	0.00%	3	0.85%	0	0.00%	Kallotenuales	Chloroflexi
0	0.00%	0	0.00%	6	1.88%	C0119	Chloroflexi
0	0.00%	1	0.28%	0	0.00%	Rickettsiales	Proteobacteria (alpha)

Supplementary Table 2.1: Estimation of Microbial Growth:

$N_{TOTALi(0)} = N_{LIGHTi(0)}$	At time 0, the total abundance of 16S rRNA gene copies (N_{TOTAL}) for a single taxon (*i*) is equivalent to the abundance of unlabeled 16S rRNA gene copies at the beginning of the incubation.
$N_{TOTALi(t)} = N_{LIGHTi(t)} + N_{HEAVYi(t)}$	By the end of the incubation period, both unlabeled and labeled 16S rRNA gene copies may have been present.
$N_{TOTALi(t)} = N_{TOTALi(0)} \times e^{ri(t)}$	For each bacterial taxon (*i*), I assumed that the abundance of cells at time *t* was proportional to the total abundance of 16S rRNA gene copies, and that changes in bacterial abundances followed an exponential growth model over the 7-d incubation period,with the net rate of population growth (*ri*). Taxon-specific abundances of 16S rRNA gene copies (N_{TOTALi}) before and after incubation were calculated as the products of the total abundance of 16S rRNA gene copies across all taxa, determined by qPCR, and the relative abundance of 16S rRNA gene copies associated with taxon, determined by sequencing.
$N_{LIGHTi(t)} = N_{TOTALi(t)} \times (M_{HEAVYi} - M_{LABi}) / (M_{HEAVYi} - M_{LIGHTi})$	I then used a linear mixing model of DNA molecular weights to estimate the abundance of labeled 16S rRNA gene copies at the end of the incubation ($N_{HEAVYi(t)}$). and by difference, $N_{LIGHTi(t)}$. Where for each taxon (i),$N_{TOTALi(t)}$ is the total (labeled+unlabeled) abundance of 16S rRNA gene copies at the end of the incubation, where M_{HEAVYi} is the molecular weight of ^{15}N-labeled DNA, M_{LIGHTi} is the molecular weight of unlabeled DNA, and M_{LABi} is the average molecular weight of DNA (labeled+unlabeled) at the end of the $^{15}NH_4$ incubation.

Chapter 3: The impact of nitrogen deposition on the desert soil bacterial metagenome: connecting taxonomy to nitrogen cycling gene inventory

Introduction

The aim of this chapter is to determine how N-dep is changing the inventory of genes that transform and emit nitrogen (N) by altering the composition of soil bacteria. Because most soil ecosystems are N-limited, added N increases denitrification genes in the gene inventory by relieving substrate limitation. In grasslands, N-dep increases the abundance of denitrification genes *nirK* and *nosZ*, the bacterial ammonia oxidizing gene *amoA,* and microbial biomass growth following rewetting (Ning et al 2015; Wang et al 2020). In forest soils, N-dep increases genes for nitrosative stress in addition to denitrification genes, which may lead to N loss from the system by leaching and gas emissions (Freedman et al 2016b). Added soil N has opposite effects on the abundances of genes encoding the different denitrifying enzyme isoforms like *nirK*/*nirS* and *cNor*/*qNor* (Nadeau et al., 2019).

Denitrification is not an essential physiological trait for any organism (Shapleigh, 2012) and is therefore not associated with any one phylogenetic group nor associated with any clear phylogenetic patterns (Graf et al., 2014). Therefore, it is likely that nitrogen deposition impacts the composition of denitrifying genes at high order levels of soil microbiome organization. Nitrogen deposition influences soil metabolism through changes to composition of soil bacteria at high levels, including Phylum-level composition and even gram-negative (G−) / gram-positive (G+). By creating easier access to NO_3, N-dep may change the balance G- abundance and G+ bacteria indirectly by decreasing the amount of belowground C allocation as G+ bacteria can use more recalcitrant C fractions while G− bacteria rely on readily degradable plant C sources

(Hoberg et al 2007, Kramer and Gleixner 2008). N-dep also changes the balance of bacterial copiotrophs and oligotrophs by increasing the amount of Proteobacteria and Bacteroidetes clades relative to Acidobacteria (Fierer et al 2012).

The metabolic strategy of soil bacteria may be an important factor for nitrogen deposition response by nitrogen availability influence catabolic, biomass-building processes. As discussed in the previous chapter, added N relieves substrate limitation on N-limited assimilatory processes: Increased availability of nitrogen turns on the transcription of ammonia consuming, amino acid synthesizing genes such as *glnA* and *asnB* (Reyes et al 1997). However, there is a difference between a single dose of extra nitrogen and chronic (high annual) exposure to nitrogen deposition on substrate limitation. In forest soils for example, microbial biomass and richness increased with N treatment in sites receiving low annual N-dep, but decreased in sites with high ambient deposition (Moore et al 2021).

In several contexts, nitrogen deposition seems to activate bacterial metabolism, but still may have an overall negative effect on total microbial activity and biomass due it's opposite effects on fungal metabolism. Nitrogen deposition changes how carbon is decomposed by increasing decomposing activities by bacteria, including higher expression of C-degrading bacterial over fungal enzymes (Freedman et al 2016a) and increasing network connectivity between bacterial decomposers (Freedman et al 2015). Adding N to soils decreases abundance of fungi responsible for lignin decomposing enzyme activity, which can explain why nitrogen deposition can cause buildup of organic matter over time (Morrison et al 2018). Fungal biomass and activity may be decreased with N-dep due to their nitrosative stress response to the production of nitrogenous intermediate compounds like NO and nitric acid (Canovas et al 2016).

For this chapter, I collected soils from across an N-dep gradient and sequenced metagenome from dry and nitrogen incubated soils in order to determine how chronic exposure to nitrogen deposition impact the nitrogen transformation strategies of desert soil bacteria. My hypotheses for this experiment are:

1. N-dep will change the composition of nitrogen cycling genes by increasing the denitrifying inventory. I expect that with higher inputs of NO_3 and NH_4 due to N-dep, respiration through denitrification will increase and there will be a higher abundance of microbial genomes containing genes for nitrate, nitrite, nitric oxide and nitrous oxide reductases.
2. The inventory of denitrifying genes will increase due to the selection of specific denitrifying clades by N-dep conditions. N-dep has been shown to impact Phylum-level organization of the soil microbiome, often increasing the ratio of Proteobacteria and Bacteroidetes to Actinobacteria and Acidobacteria, therefore I predict that soils receiving more N-dep will have more denitrifying genes due to the higher abundance of these taxa.

Methods

Study Sites & Experimental Design: This experiment was performed at the 3 sites described in Chapter 2 (Pinto Basin, Wide Canyon, and Morongo Canyon) and Boyd Deep Canyon, described in Chapter 1. Rewetting experiments were performed underneath the canopies of 4 creosote shrubs at each site (n=4). Under each shrub, we installed 2 PVC collars. The collars had a diameter of 20 cm, a height of 10 cm and were inserted 5 cm into the soil at least 50 cm apart to avoid cross-contamination of treatments. One collar per shrub was rewet with 500 mL of deionized water (water only control) and the other collar was rewet with a solution of NH_4 in 500 mL of deionized water. Soils were sampled < 1 hour before rewetting and 24 hours post rewetting to capture changes occurring during the rewetting induced burst of microbial activity. At Pinto Basin, there was a summer monsoonal event that interrupted our field experiment

Metagenome library prep and sequencing: DNA was extracted from each soil sample using the PowerLyzer PowerSoil DNA Isolation Kit according to the manufacturer's instructions, with an additional initial 25-min incubation at 65°C to aid in lysing cells. DNA extracts were then analyzed for quality using nanodrop and gel electrophoresis, quantified using a QuBit fluorometer, and sent to the QB3 genomics facility at the University of California, Berkeley. At QB3, samples were prepped into a shotgun metagenomics library and sequenced on the Illumina NovaSeq S1 150PE platform.

Metagenome Bioinformatics: Reads were analyzed using the metaWrap pipeline (Uritskiy et al., 2018): Raw reads were pre-processed using the default settings of trim-galore to remove low quality sequences based on phred score. Trimmed reads were then assembled using MegaHit to produce contigs 1000bp and over. One assembly was

performed per site. Assembled contigs were then binned into genomic bins using metaWrap's binning workflow which includes creating binsets with three algorithms (MaxBin2, metaBAT2, and CONCOCT), combining the 3 separate bins sets, and reassembling with any reads that align to the new bin set. The abundance of each genomic bin in each sample was then determined using the Salmon algorithm. The taxonomy of each genomic bin was determined by using MegaBLAST against the NCBI_nt database. Functional genes were annotated in genomic bins using PROKKA v1.12. Annotation outputs from this pipeline include the COG identification number, eC number, gene name and gene product for each open reading frame. A summary of the functional gene annotations for each site is provided in Supplementary Table 3.1. Annotated genes were then subset to microbial functions relevant to the soil nitrogen cycle using the gene list from Ncycdb along with additional manual curation and refinement (Tu et al., 2018).

Statistical analysis: Analysis of the taxonomic composition of bins and functional annotations across sampling sites were performed on relative abundances using Principal Component Analysis (PCA). Statistical testing of compositional differences was performed using PERMANOVA on euclidean distance matrices. Statistical testing on the effect of rewetting treatment and nitrogen addition on the mean abundance of specific bacterial orders and gene groups was performed using ANOVAs accounting for error across biological replicates (shrubs).

Results

Review of binning results: In total, I found 768 bins across the 4 sampling sites. At Pinto Basin I recovered 118 bins, 240 at Boyd Deep Canyon, 193 at Wide Canyon, and 217 at Morongo Canyon. Bins represent partially sequenced fragments (here, a cutoff of at least 10% completion was used) of full bacterial genomes. Abundance values were calculated as genome copies per million reads for each bin using the Salmon algorithm (Patro et al., 2017) within the metaWrap pipeline. The abundance of a functional gene in one sample is therefore expressed as the sum of abundances of all the bins containing that gene. For the rest of this chapter, genomic bins will be referred to as genomes.

Taxonomic composition of genomes across N-deposition gradient: I recovered bins from 5 bacterial Phyla: the Proteobacteria, Actinobacteria, Bacteroidetes, Gemmatimonadetes, and Planctomycetes. I also recovered bins from one archaeal Phylum, the Thaumarchaeota. Approximately 90 of the bins could not be assigned a Phylum with the taxator-tk algorithm despite the assembled genomes ranging from approximately 0.4-2 million base pairs. Of the 30 identified orders, 11 orders belonged to the Proteobacteria phylum and 9 to the Actinobacteria phylum. Principal component analysis on order-level composition of bacterial genomes indicated that taxonomic composition of soil genomes is geographically correlated with annual nitrogen deposition (Fig. 3.1) [PERMANOVA $F=20.391$, $p=0.002$]. Specifically, with increasing N-dep, there is increased abundance of the Proteobacteria, Actinobacteria, Gemmatimonadetes, Planctomycetes, and Bacteroidetes. Some orders of Proteobacteria and Actinobacteria also decreased with N-deposition.

Response of genome abundance to rewetting: Analysis of the effect of composition over time and in response to nitrogen indicated only Morongo Canyon had a significant overall composition shift of genomes in response to rewetting [PERMANOVA F=1.195, p=0.04]. However, I also ran individual ANOVAs on all of the genomes over time and in response to nitrogen addition, and I found that the abundance of individual genomes was significantly affected by rewetting and nitrogen treatments. At Pinto Basin, 9 genomes were impacted by rewetting. At Boyd Canyon, 41 genomes were impacted by rewetting and 20 by rewetting with nitrogen. At Wide Canyon, 16 by rewetting and 46 by rewetting with nitrogen. Lastly at Morongo Canyon, 16 genomes were affected by rewetting and 17 by rewetting with nitrogen. There was not a relationship between N-dep and the total number or percent of genomes responsive to rewetting or nitrogen treatments.

In Figure 3.2, I visualized the mean of pre- and post-rewetting abundances for each bin in order to visualize order-level abundance patterns across the N-dep gradient. Of the 30 taxonomic orders found, the 4 most abundant orders were the Actinobacterial clades Geodermatophilales (8.7% of genomes) and Rubrobacterales (10.6% of genomes), and the Proteobacterial clades Hyphomicrobiales (12.5% of genomes) and Sphingomonadales (6.11% of genomes). These clades contained a large proportion of the genomes that significantly increased or decreased in abundance in response to rewetting, except for the Rubrobacterales. While there were no taxonomic patterns of rewetting response across the N-dep gradient, there was a significant impact of N-dep on the average total abundance of these 4 Orders (Fig. 3.3). Specifically, N-dep was significantly positively correlated with the abundance of Sphingomonadales [ANOVA F=55.707, p=6e-8] and negatively correlated with the abundance of the Rubrobacterales

[ANOVA F=23.714, p=4.-5], Geodermatophilales [ANOVA F=19.700, p=1e-4], and the Hyphomicrobiales [ANOVA F=56.800, p=5e-8].

Composition of nitrogen-cycling genes across N-deposition gradient: I searched the functional annotations of the recovered genomes for genes relevant to soil nitrogen cycling using the list of genes from the specialized database Ncycdb (Tu et al., 2018) along with manual curation and refinement of recovered annotations. A summary of the nitrogen cycling genes found in these genomes is summarized in Table 1. Notably, I did not find any annotation for ammonia monooxygenase (*amo*) despite recovering genomes from the putative archean ammonia-oxidizing clade, Nitrososphaerales.

To determine the impact of nitrogen deposition on the composition of these nitrogen cycling genes, I then ran a principal component analysis on annual N-dep and the abundance of recovered nitrogen cycling genes (Fig. 3.4). I found that N-dep significantly predicted the composition of N-cycling genes [PERMANOVA F=14.601, p=0.002], covarying the most with genes belonging to the denitrification, dissimilatory nitrate reduction to ammonia, and organic degradation/synthesis pathways. ANOVA on linear regression between nitrogen deposition and abundance of genomes containing N-cycling genes shows that N-dep decreases the abundance genes associated with nitrate reductase *nap* [F=15.339 p=1e-4], nitrite reductase *nrf* [F=3.788 p=0.04], and nitrous-oxide reductase *nos* [F=548.30, p=2e-6]. The only denitrifying gene that increased in abundance with increasing N-dep was nitrite reductase *nir* [F=18.003 p=5e-5]. N-dep also decreased the abundance of the NH_4-consuming amino acid synthetase, glutamine synthetase *gln* [F= 46.252, p=4e-8] (Fig. 3.5).

Connecting nitrogen cycling inventory to taxonomic composition: Although nitrogen deposition increased the abundance of genomes containing nitrite reductase

nir, there were no *nir* genes found in the Sphingomonadales, the only taxonomic group that significantly increased with N-deposition. Nitrite reductase *nir* was found in 42 genomes total, with 67% of those genomes belonging to the actinobacterial Phylum, including many genomes unclassified at the order level or below. Genomes containing *nir* genes that could be assigned taxonomy at the genus level included Proteobacteria *Massilia, Microvirga, Pseudomonas*, and Actinobacteria *Kocuria* and *Modestobacter.*

Nitrate reductase *nap* and nitrite reductase *nrf* were found in 78 and 37 genomes, respectively. Approximately 12% of the *nap* containing genomes belonged to the Rubrobacterales order, so the abundance of periplasmic nitrate reductase in the nitrogen cycling inventory decreased due in part to the suppression of this specific clade by nitrogen deposition. The *nrf* gene was mostly found in the genomes of Proteobacteria or bacteria that could not be assigned a Phylum, although it was not more frequent in any one order. Genomes containing *nrf* genes that were assigned at the genus level include the Proteobacteria *Archangium*, *Methylobacterium*, *Pseudomonas*, and the Actinobacteria *Rubrobacter*.

Discussion & Conclusions

Nitrogen deposition impacted the nitrogen cycling gene inventory by decreasing the abundance of genomes containing one type of nitrite reductase, *nrf,* and increasing the abundance of genomes containing another nitrite reductase, *nir.* The difference between these two nitrite reductases is that *nir* reduces NO_2- to NO as part of the denitrification pathway while *nrf* transforms $NO_3$and formate into NH_4 (Mohan et al., 2004) during dissimilatory nitrate reduction to ammonium (DNRA). Multiple studies in agricultural soils have concluded that DNRA and denitrification are competitive processes and balance between them will determine the conservation or gaseous loss, respectively, of nitrogen from the system based on the observation that NH_4 generated by DNRA remains in the soil when it is assimilated into biomass (Bhowmik et al., 2017; Putz et al., 2018; Yoon et al., 2019). Nitrogen deposition altering the balance of *nir* and *nrf* could be a key mechanism underlying the effects of N-dep on soil N emissions, although an flux measurement experiment conducted along this same N-dep gradient (Eberwein et al., 2020) found higher NO_x and N_2O losses post-rewetting at Boyd Canyon compared to a higher N-dep site.

What could be the mechanism for this impact of chronic atmospheric nitrogen deposition on the ratio of *nrf*:*nir* in desert soils? Culture studies in E. coli containing both of these nitrite reductase types has shown that the *nir* operon is upregulated when excess NO_3 is in the cell's environment, while *nrf* is active at low NO_3 conditions only (H. Wang & Gunsalus, 2000). Therefore, it is possible that deposition of mineral N onto the soil could be selecting for bacteria with *nir* genes over *nrf* genes if *nir* has a higher affinity for NO_2 substrate when soil NO_3 levels are high. A meta analysis by (Pandey et al., 2020) found that abundance of *nrf* genes in soil ecosystems is positively correlated

to the ratio of soil carbon to NO_3. In culture, certain carbon sources consistently favor DNRA while others favor denitrification (Carlson et al., 2020). (Vuono et al., 2019) elaborated on this theory, postulating that *nrf* is sensitive to carbon or nitrogen limitation due to the high energetic cost of the protein compared to *nir*, and that DNRA can still be active at low C:N ratios as long as neither is limiting.

I could not detect an effect of N-dep in either rewetting treatments or nitrogen addition from this experiment. Neither the taxonomic identity or number of genomes changing with treatment was influenced by nitrogen deposition, however this may be due to the limitation of this analysis to reads binned into genomes with a cutoff for genome completion, which could less abundant taxa could be more affected by N-dep. At all sites, the two dominant Proteobacterial orders, Sphingomonadales and Hyphomicrobiales, were the most rewetting activated clades, and N-dep did increase the overall abundance of proteobacterial genomes. Therefore, it could be possible that in this desert system, where biochemical pulses make up a significant proportion of total bacterial metabolism, proteobacteria are capable of gaining the advantage in soils with higher N loads specifically during the immediate period following rewetting. This may be more linked to proteobacterial copiotrophic growth strategies and the ability to grow on mineral N than denitrification.

These results show that nitrogen deposition increased the abundance of Sphingomonadales bacteria in desert soil. The Sphingomonadales order of bacteria are widespread in soil environments, but dominate in hot desert desert soils (Lester et al., 2007; Zhang et al., 2016), soil disturbed by agricultural use (Wolińska et al., 2018) and even in the rhizospheres of high altitude plant communities (Angel et al., 2016). Although the Sphingomonadales found in these soils do not seem to be responding to nitrogen

deposition via their denitrifying genes (i.e., they do not contain any *nir*), their increasing abundance in response to N-deposition indicates that they are sensitive in some way to the availability of mineral N, which is also supported by their agricultural and other disturbed soil environments. Although I could not assign taxonomy below the family level to any of the Sphingomonad bacteria in these soils, other genera within this order have distinguishing characteristics including the ability to fix nitrogen, tolerate drought conditions, and degrade lignocellulose and polyaromatic hydrocarbons (Asaf et al., 2020).

In conclusion, the results of this experiment show that nitrogen deposition alters the soil microbiome in desert ecosystems by changing both the composition of microbial genomes and the abundance of nitrogen cycling genes. N-dep increased the abundance of denitrifying NO_2 reducing genes (*nir*) while decreasing DNRA NO_2- reducing genes (*nrf*), potentially due to the excess of available NO_3. The decreasing abundance of genes encoding the periplasmic nitrate reductase enzyme (nap) was lower across the N-dep gradient due to the decreased abundance of the dominant Actinobacterial order, Rubrobacterales. However, not all changing patterns of functional genes were tied to the abundance of specific taxa. The abundance of *nir* genes with increasing N-dep is due to the increase in Proteobacteria, but was not linked to any specific lower taxonomic levels. Likewise, the *nrf* gene occurred more in both Proteobacterial and Actinobacterial clades but was not more abundant due to one specific group.

Figures & Tables

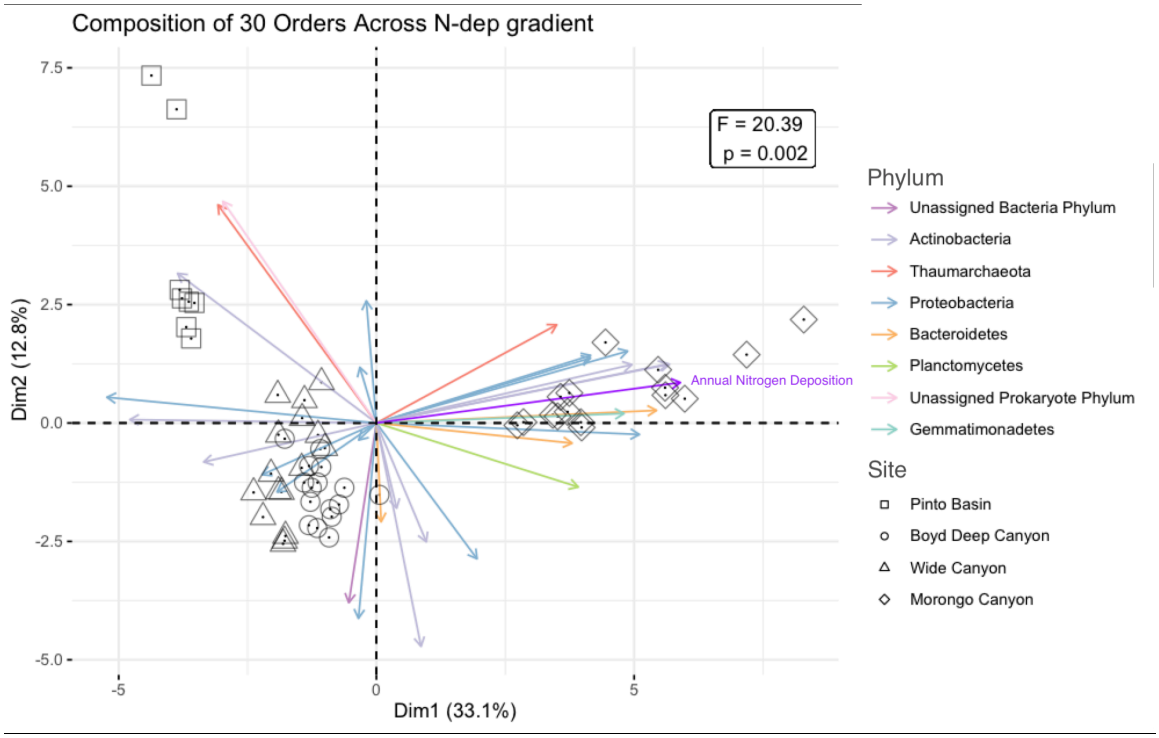

Figure 3.1: Impact of Nitrogen Deposition on Taxonomic Composition of Recovered Genomes. Principal coordinate analysis was performed on relative abundances of genomes merged at the order level. Each arrow represents a bacterial order and the arrows are colored by Phylum. Annual nitrogen deposition rate was included in the ordination (bright purple arrow) to determine which order abundances were most correlated with N-dep. The impact of site on Order level composition was tested with a PERMANOVA, and results of this model is show in the box.

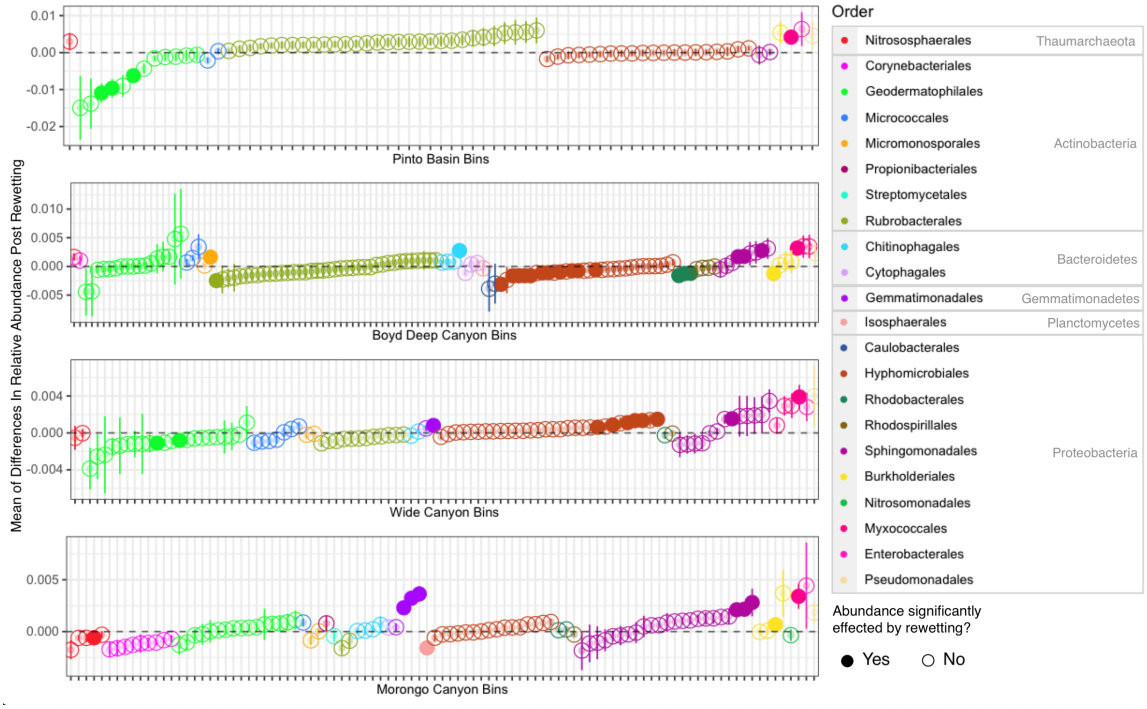

Figure 3.2: Post-Rewetting Changes in Genome Abundance. I plot the mean of post-rewetting abundance change for each genome at each site. Error bars indicate the mean of differences +/- one standard error. Points are colored by order, and the color key on the right hand side is ordered by Phylum. Solid points have statistically significant post-rewetting abundance differences.

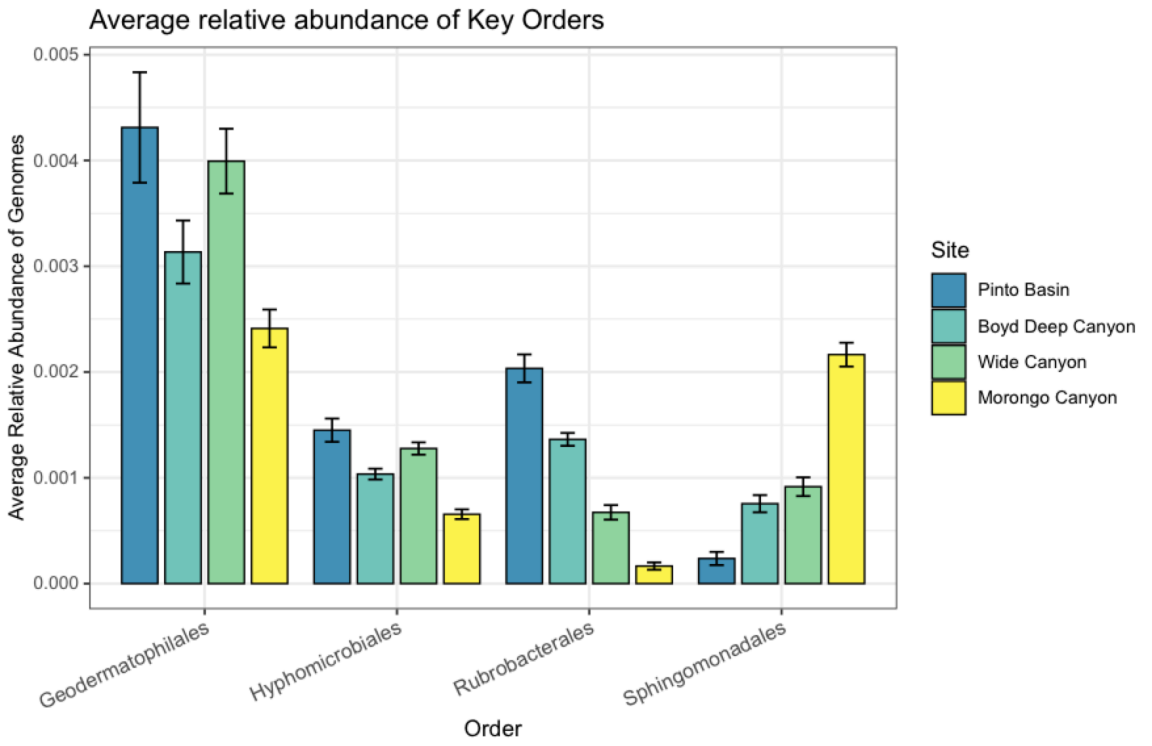

Figure 3.3: Differential Abundance of 4 Key Bacterial Orders Across Nitrogen Deposition Gradient. The following 4 orders were found to have abundance significantly correlated to annual nitrogen deposition rate. Bars represent the mean relative abundance of genome with each order at each site +/- one standard error.

Table 3.1: Inventory of nitrogen cycling genes found in desert soils.

gene group	recovered genes	Key enzyme	substrate	product	associated N cycle process
hzs	*hzsA, hzsB, hzsC*	Hydrazine synthase	NO_2 + NH_4	N_2H_2	Anammox
nos	*nosZ*	Nitrous-oxide reductase	N_2O	N_2	Denitrification
nor	*norB, norC*	Nitric oxide reductase	NO	N_2O	Denitrification
ani	*aniA*	Copper-containing nitrite reductase	NO_2	NO	Denitrification
nir	*nirD, nirK*	Nitrite reductase	NO_2	NO_2	Denitrification
nap	*napA, napB, napC, napD, napE, napF*	Nitrate reductase	NO_3	NO_2	Denitrification
nar	*narB, narG, narH, narI, narJ, narK, narL, narQ, narT, narU, narW, narX, narY, narZ*	Nitrate reductase	NO_3	NO_2	Denitrification
hao	*hao*	Hydroxylamine dehydrogenase	NH_2OH	NO_2, NO	Nitrification
nrf	*nrfA, nrfG, nrfH*	Nitrite reductase	NO_3	NH_4	Dissimilatory nitrate reduction to Ammonium
nrt	*nrtA, nrtP*	Nitrate/nitrite transporter	NO3, NO2		Dissimilatory nitrate reduction to Ammonium
fdn	*fdnG, fdnH, fdnI, fnr*	Nitrate-dependant Formate dehydrogenase	CHO_2 + NO_3	NO_2	Organic degradation and synthesis
ure	*ureA, ureB, ureC, ureD, ureE, ureF, ureG, ureH, ureI, ureR*	Urease	$CO(NH_2)_2$	NH_4	Organic degradation and synthesis
hcp	*hcp*	Hydroxylamine reductase	NH4	NH2OH	Organic degradation and synthesis
gln	*glnA*	Glutamine synthetase	NH4	Organic C	Organic degradation and synthesis
asn	*asnB*	Asparagine synthase	NH4	Organic N	Organic degradation and synthesis
nas	*nasA, nasB, nasC, nasR*	Assimilatory nitrate reductase	NO3	Organic N	Organic degradation and synthesis
ans	*ansB*	Asparaginase	Organic N	NH4	Organic degradation and synthesis
gls	*glsA*	Glutaminase	Organic N	NH4	Organic degradation and synthesis
amt	*amt, amtB*	Ammonia transporter	NH4		Transport
nif	*nifD, nifH, nifW*	Nitrogenase	N_2	NH_4	Nitrogen fixation

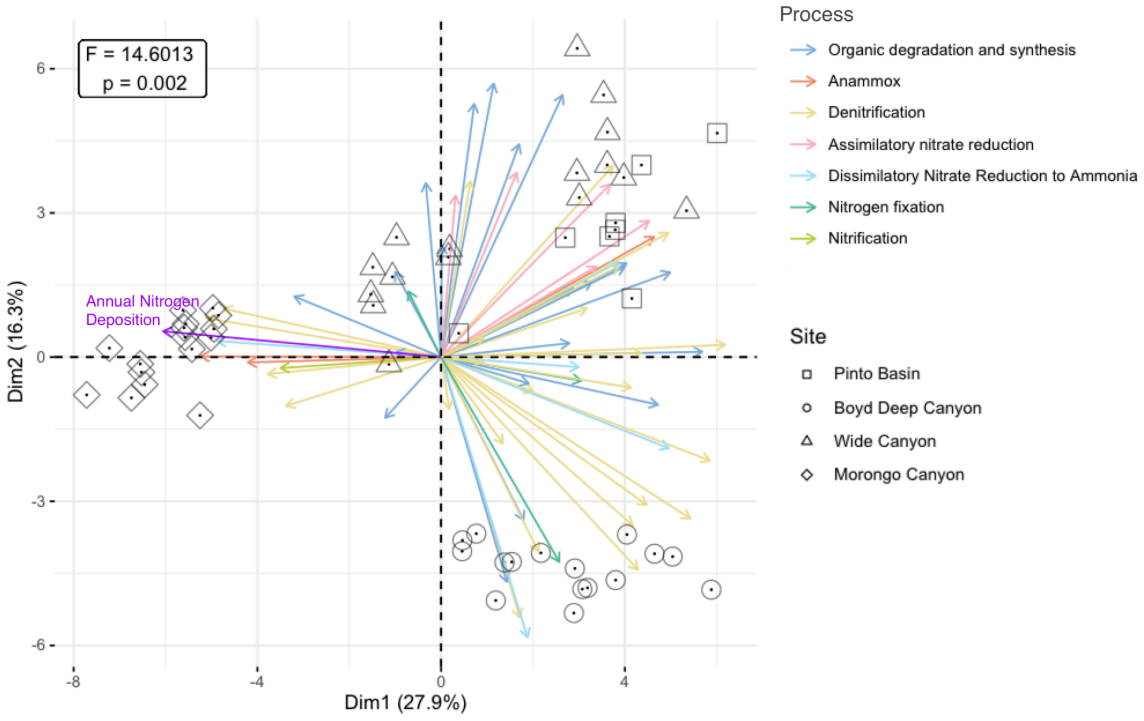

Figure 3.4: Impact of Nitrogen Deposition on Composition of Nitrogen-Cycling Functional Genes. Principal coordinate analysis was performed on relative abundances of nitrogen cycling genes. Each arrow represents a gene recovered from functional annotation and the arrows are colored by nitrogen cycling process determined from Ncycdb. Annual nitrogen deposition rate was included in the ordination (bright purple arrow) to determine which genes were most correlated with N-dep. The impact of site on gene composition was tested with a PERMANOVA, and results of this model is show in the box.

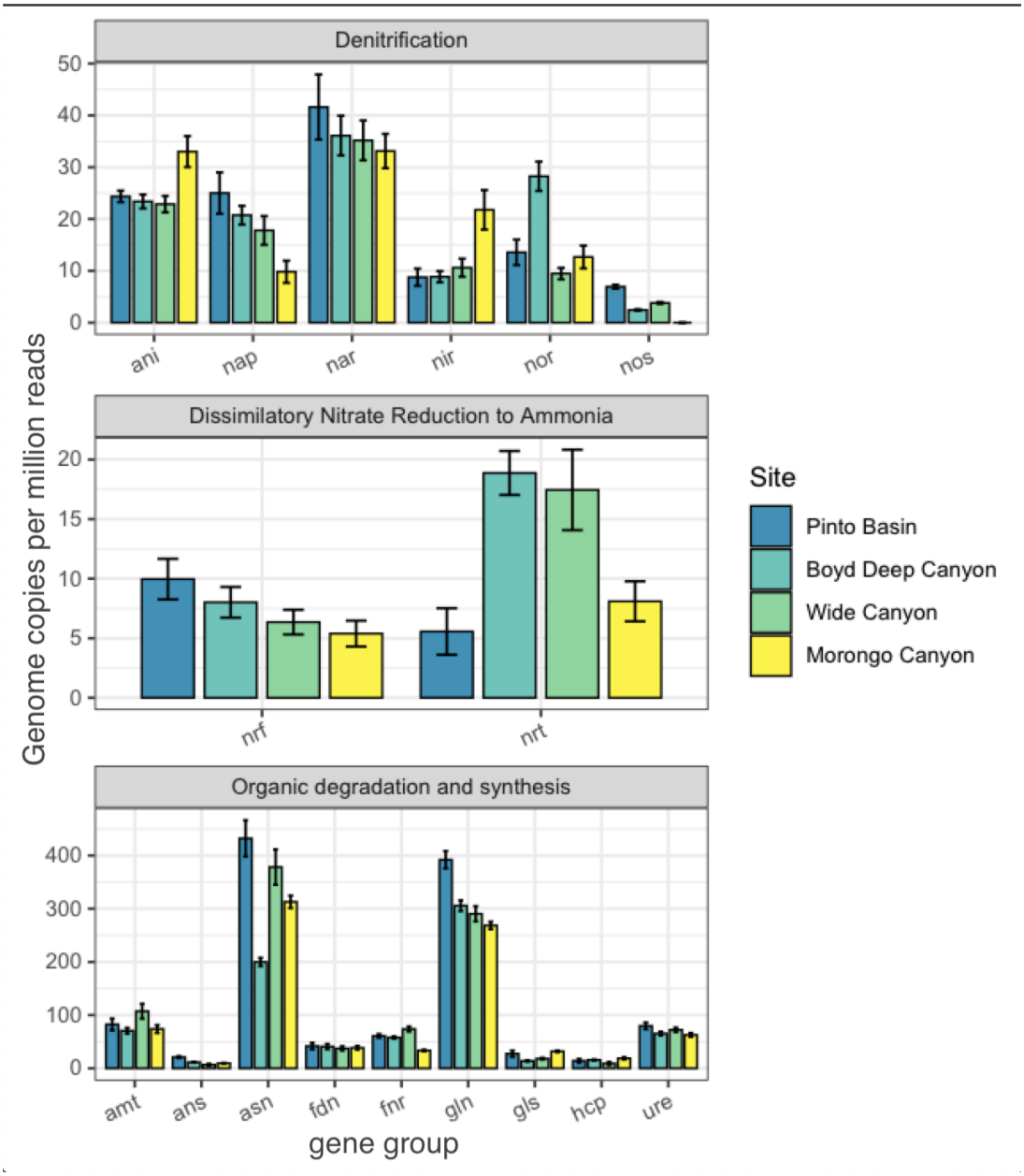

Figure 3.5: Impact of Nitrogen Deposition on Nitrogen Cycling Functional Gene Abundance. The following nitrogen cycling processes were found to contain genes with differential abundance across the N-dep gradient. The mean abundance of genomes containing each nitrogen cycling gene was plotted with error bars representing +/- 1 standard error.

Supplementary Table 3.1: Functional annotation results from MetaWrap pipeline.

Site	Hypothetical Proteins	Non-hypothetical proteins	Non redundant genes	Non redundant products	Unique COGs	Unique eCs
PB	120,108	74,762	12,896	6,852	2,260	2,111
BC	268,908	178,508	16,792	7,540	2,297	2,284
MC	243,879	160,569	16,339	7,776	2,317	2,337
WC	194,055	131,769	15,583	7,509	2,313	2,277
All	•	545,608	22,046	8,601	2,454	2,433

Synthesis & Final Conclusions

Observations of soil microbiomes under nitrogen deposition have suggested that increased N-dep alters the balance between fungal and bacterial growth and metabolism. My results support this conclusion: Bacterial communities responded more than fungi to NO_3 addition during a rewetting pulse (Chapter 1), and I characterized a diverse community capable of assimilating NH_4 with phylogenetic diversity increasing with N-dep (Chapter 2). Therefore, N-dep may favor bacterial metabolism due to relieving direct substrate limitation of microbial growth processes using simple mineral N as opposed to microbes capable of directly assimilating organic forms of N. If there is a shift away from bacteria able to directly uptake organic forms of N (e.g. amino acids), this may have consequences for plant microbial-interactions: microbes that directly uptake NH_4 compete with plants for nitrogen will organic N assimilators do not (Geisseler et al., 2010). Higher availability of NH_4 may also impact the greater decomposer network, since when NH_4 level are high, microbes produce fewer extracellular hydrolases that mineralize N from organic matter due to the high metabolic cost of creating these enzymes.

In chapter 2, I found evidence for shifting taxonomic groups across the N-dep gradient that may represent different nitrogen assimilation strategies. The most evident shift was decreased number of Hyphomicrobiales incorporators and increased abundance of Sphingomonadales and Blastocatellales incorporators. Future research into the nitrogen mineralizing gene inventories of these orders could shed light on the metabolic drivers behind these clades responses to N-dep. While these specific taxonomic groups were affected, N-dep also broadly increased the phylogenetic diversity of NH_4 assimilators, potentially suggesting that in addition to changing the abundance of

specific groups, higher available N could be influencing more taxa to grow on the freely available NH_4 instead of producing exoenzymes. In California grasslands, however N-dep was found to alter some exoenzyme abundances but not N-mineralizing enzymes (Vourlitis et al., 2021).

At the moderately low N-dep site Boyd Deep Canyon, I found evidence that gross changes in the fungal community were correlated with NO emissions, suggesting that fungal denitrification may dominate over bacterial. Fungal composition also did not change with NO_3 addition, indicating that fungal growth post rewetting was not N-limited. This evidence for fungal denitrification in low N-dep soil could suggest that any effect of N-dep on N emissions could be related to lower denitrification compared to bacterial denitrification. Furthermore, in chapter 3 I found increased abundance of bacterial denitrification genes, although functional gene analysis was restricted to prokaryotes.

Finally, stable isotope experiments in chapters 1 and 3 support the growing body of evidence that only a subset of taxa detected with 16S gene sequencing are active during rewetting pulses. About ⅓ and ¼ of taxa identified in the 16S sequences were actively growing using $H_2{}^{18}O$ and $^{15}NH_4$ probes, respectively. Among those groups, Proteobacteria and Actinobacteria were dominant. These results suggest that a majority of taxa are inactive during rewetting pulses, or have such a low level of biomass and activity they can't be detected. This supports the theory of many ASVs identified using sequencing data being dormant or relic DNA.

References

Abed, Raeid M. M., Phyllis Lam, Dirk de Beer, and Peter Stief. 2013. “High Rates of Denitrification and Nitrous Oxide Emission in Arid Biological Soil Crusts from the Sultanate of Oman.” *The ISME Journal* 7 (9): 1862–75.

Aldossari, Nouf, and Satoshi Ishii. 2021. “Fungal Denitrification Revisited – Recent Advancements and Future Opportunities.” *Soil Biology & Biochemistry* 157 (June): 108250.

Andrews, Holly M., and G. Darrel Jenerette. 2020. “Exotic Grass Litter Modulates Seasonal Pulse Dynamics of CO2 and N2O, but Not NO, in Mediterranean-Type Coastal Sage Scrub at the Wildland-Urban Interface.” *Plant and Soil* 456 (1): 339–53.

Angel, Roey, Ralf Conrad, Miroslav Dvorsky, Martin Kopecky, Milan Kotilínek, Inga Hiiesalu, Fritz Schweingruber, and Jiří Doležal. 2016. “The Root-Associated Microbial Community of the World’s Highest Growing Vascular Plants.” *Microbial Ecology* 72 (2): 394–406.

Armstrong, Alacia, Angel Valverde, Jean-Baptiste Ramond, Thulani P. Makhalanyane, Janet K. Jansson, David W. Hopkins, Thomas J. Aspray, Mary Seely, Marla I. Trindade, and Don A. Cowan. 2016. “Temporal Dynamics of Hot Desert Microbial Communities Reveal Structural and Functional Responses to Water Input.” *Scientific Reports* 6 (September): 34434.

Averill, Colin, Michael C. Dietze, and Jennifer M. Bhatnagar. 2018. “Continental-Scale Nitrogen Pollution Is Shifting Forest Mycorrhizal Associations and Soil Carbon Stocks.” *Global Change Biology* 24 (10): 4544–53.

Baidya, Sachin, Jeffrey W. Cary, W. Scott Grayburn, and A. M. Calvo. 2011. “Role of Nitric Oxide and Flavohemoglobin Homolog Genes in Aspergillus Nidulans Sexual Development and Mycotoxin Production.” *Applied and Environmental Microbiology* 77 (15): 5524–28.

Baselga, Andrés, and C. David L. Orme. 2012. “Betapart : An R Package for the Study of Beta Diversity.” *Methods in Ecology and Evolution / British Ecological Society* 3 (5): 808–12.

Bedmar, E. J., E. F. Robles, and M. J. Delgado. 2005. “The Complete Denitrification Pathway of the Symbiotic, Nitrogen-Fixing Bacterium Bradyrhizobium Japonicum.” *Biochemical Society Transactions* 33 (Pt 1): 141–44.

Belnap, J. 1995. “Surface Disturbances: Their Role in Accelerating Desertification.” *Environmental Monitoring and Assessment* 37 (1-3): 39–57.

Bhowmik, Arnab, Mara Cloutier, Emily Ball, and Mary Ann Bruns. 2017. “Underexplored Microbial Metabolisms for Enhanced Nutrient Recycling in Agricultural Soils.” *AIMS Microbiology* 3 (4): 826–45.

Blazewicz, S. J., E. Schwartz, and M. K. Firestone. 2014. “Growth and Death of Bacteria and Fungi Underlie Rainfall‐induced Carbon Dioxide Pulses from Seasonally Dried Soil.” *Ecology*. https://esajournals.onlinelibrary.wiley.com/doi/abs/10.1890/13-1031.1.

Blazewicz, Steven J., Bruce A. Hungate, Benjamin J. Koch, Erin E. Nuccio, Ember Morrissey, Eoin L. Brodie, Egbert Schwartz, Jennifer Pett-Ridge, and Mary K. Firestone. 2020. “Taxon-Specific Microbial Growth and Mortality Patterns Reveal Distinct Temporal Population Responses to Rewetting in a California Grassland Soil.” *The ISME Journal* 14 (6): 1520–32.

Bokulich, Nicholas A., Sathish Subramanian, Jeremiah J. Faith, Dirk Gevers, Jeffrey I. Gordon, Rob Knight, David A. Mills, and J. Gregory Caporaso. 2013. “Quality-Filtering Vastly Improves Diversity Estimates from Illumina Amplicon Sequencing.” *Nature Methods* 10 (1): 57–59.

Bolyen, Evan, Jai Ram Rideout, Matthew R. Dillon, Nicholas A. Bokulich, Christian C. Abnet, Gabriel A. Al-Ghalith, Harriet Alexander, et al. 2019. “Reproducible, Interactive, Scalable and Extensible Microbiome Data Science Using QIIME 2.” *Nature Biotechnology* 37 (8): 852–57.

Butterbach-Bahl, Klaus, Elizabeth M. Baggs, Michael Dannenmann, Ralf Kiese, and Sophie Zechmeister-Boltenstern. 2013. “Nitrous Oxide Emissions from Soils: How Well Do We Understand the Processes and Their Controls?” *Philosophical Transactions of the Royal Society of London. Series B, Biological Sciences* 368 (1621): 20130122.

Cánovas, David, Jose F. Marcos, Ana T. Marcos, and Joseph Strauss. 2016. “Nitric Oxide in Fungi: Is There NO Light at the End of the Tunnel?” *Current Genetics* 62 (3): 513–18.

Carlson, Hans K., Lauren M. Lui, Morgan N. Price, Alexey E. Kazakov, Alex V. Carr, Jennifer V. Kuehl, Trenton K. Owens, Torben Nielsen, Adam P. Arkin, and Adam M. Deutschbauer. 2020. “Selective Carbon Sources Influence the End Products of Microbial Nitrate Respiration.” *The ISME Journal* 14 (8): 2034–45.

Chapelle, Emilie, Rodrigo Mendes, Peter A. H. M. Bakker, and Jos M. Raaijmakers. 2016. “Fungal Invasion of the Rhizosphere Microbiome.” *The ISME Journal* 10 (1): 265–68.

Chatterjee, A., and G. D. Jenerette. 2011. “Spatial Variability of Soil Metabolic Rate along a Dryland Elevation Gradient.” *Landscape Ecology* 26 (8): 1111.

Chen, Huaihai, Nape V. Mothapo, and Wei Shi. 2014. “The Significant Contribution of Fungi to Soil N2O Production across Diverse Ecosystems.” *Applied Soil Ecology: A Section of Agriculture, Ecosystems & Environment* 73 (January): 70–77.

Coenen, Ashley R., Sarah K. Hu, Elaine Luo, Daniel Muratore, and Joshua S. Weitz. 2020. “A Primer for Microbiome Time-Series Analysis.” *Frontiers in Genetics* 11 (April): 310.

Dictor, Marie-Christine, Laurent Tessier, and Guy Soulas. 1998. “Reassessement of the Kec Coefficient of the Fumigation–extraction Method in a Soil Profile.” *Soil Biology & Biochemistry* 30 (2): 119–27.

Ding, Yi, Donald M. Gardiner, Di Xiao, and Kemal Kazan. 2020. “Regulators of Nitric Oxide Signaling Triggered by Host Perception in a Plant Pathogen.” *Proceedings of the National Academy of Sciences of the United States of America* 117 (20): 11147–57.

Eberwein, J. R., P. M. Homyak, C. J. Carey, and E. L. Aronson. 2020. “Large Nitrogen Oxide Emission Pulses from Desert Soils and Associated Microbiomes.” *Biogeochemistry*. https://link.springer.com/article/10.1007/s10533-020-00672-9.

Eberwein, J. R., P. Y. Oikawa, L. A. Allsman, and G. D. Jenerette. 2015. “Carbon Availability Regulates Soil Respiration Response to Nitrogen and Temperature.” *Soil Biology & Biochemistry* 88 (September): 158–64.

Fenn, Mark E., Jill S. Baron, Edith B. Allen, Heather M. Rueth, Koren R. Nydick, Linda Geiser, William D. Bowman, et al. 2003. “Ecological Effects of Nitrogen Deposition in the Western United States.” *Bioscience* 53 (4): 404–20.

Fenn, M. E., E. B. Allen, S. B. Weiss, S. Jovan, L. H. Geiser, G. S. Tonnesen, R. F. Johnson, et al. 2010. “Nitrogen Critical Loads and Management Alternatives for N-Impacted Ecosystems in California.” *Journal of Environmental Management* 91 (12): 2404–23.

Fenn, M. E., S. Jovan, F. Yuan, L. Geiser, T. Meixner, and B. S. Gimeno. 2008. “Empirical and Simulated Critical Loads for Nitrogen Deposition in California Mixed Conifer Forests.” *Environmental Pollution* 155 (3): 492–511.

Fierer, Noah George. 2003. *Stress Ecology and the Dynamics of Microbial Communities and Processes in Soil*. University of California, Santa Barbara.

Fierer, Noah, and Joshua P. Schimel. 2002. “Effects of Drying–rewetting Frequency on Soil Carbon and Nitrogen Transformations.” *Soil Biology & Biochemistry* 34 (6): 777–87.

Fierer, N., and J. P. Schimel. 2003. “A Proposed Mechanism for the Pulse in Carbon Dioxide Production Commonly Observed Following the Rapid Rewetting of a Dry Soil.” *Soil Science Society of America Journal. Soil Science Society of America*. https://dl.sciencesocieties.org/publications/sssaj/abstracts/67/3/798.

Freedman, Zachary B., Rima A. Upchurch, Donald R. Zak, and Lauren C. Cline. 2016. “Anthropogenic N Deposition Slows Decay by Favoring Bacterial Metabolism: Insights from Metagenomic Analyses.” *Frontiers in Microbiology* 7. https://doi.org/10.3389/fmicb.2016.00259.

Frey, Beat, Monique Carnol, Alexander Dharmarajah, Ivano Brunner, and Patrick Schleppi. 2020. “Only Minor Changes in the Soil Microbiome of a Sub-Alpine Forest After 20 Years of Moderately Increased Nitrogen Loads.” *Frontiers in Forests and Global Change* 3. https://doi.org/10.3389/ffgc.2020.00077.

Frostegård, Åsa, Silas H. W. Vick, Natalie Y. N. Lim, Lars R. Bakken, and James P. Shapleigh. 2020. “Linking Meta-Omics to the Kinetics of Denitrification Intermediates Reveals pH-Dependent Causes of N2O Emissions and Nitrite Accumulation in Soil.” *Cold Spring Harbor Laboratory*. https://doi.org/10.1101/2020.11.26.399899.

Geisseler, Daniel, William R. Horwath, Rainer Georg Joergensen, and Bernard Ludwig. 2010. "Pathways of Nitrogen Utilization by Soil Microorganisms – A Review." *Soil Biology & Biochemistry* 42 (12): 2058–67.

González, P. J., C. Correia, Isabel Moura, C. D. Brondino, and J. J. G. Moura. 2006. "Bacterial Nitrate Reductases: Molecular and Biological Aspects of Nitrate Reduction." *Journal of Inorganic Biochemistry* 100 (5-6): 1015–23.

Haridas, S., R. Albert, M. Binder, J. Bloem, K. LaButti, A. Salamov, B. Andreopoulos, et al. 2020. "101 Dothideomycetes Genomes: A Test Case for Predicting Lifestyles and Emergence of Pathogens." *Studies in Mycology* 96 (June): 141–53.

Harris, E., E. Diaz-Pines, E. Stoll, M. Schloter, S. Schulz, C. Duffner, K. Li, et al. 2021. "Denitrifying Pathways Dominate Nitrous Oxide Emissions from Managed Grassland during Drought and Rewetting." *Science Advances* 7 (6). https://doi.org/10.1126/sciadv.abb7118.

He, Ye, Mei Hong, Xuehui Xu, Zhiwei Liang, Na Jiang, Nare Tu, and Zhendan Wu. 2022. "Nitrogen Deposition Changes the Keystone Taxa of Soil Microorganisms and Indirectly Affects Plant Aboveground Biomass in Desert Steppe Regions." https://www.researchsquare.com/article/rs-1354926/latest.pdf.

Higgins, Steven A., Allana Welsh, Luis H. Orellana, Konstantinos T. Konstantinidis, Joanne C. Chee-Sanford, Robert A. Sanford, Christopher W. Schadt, and Frank E. Löffler. 2016. "Detection and Diversity of Fungal Nitric Oxide Reductase Genes (p450nor) in Agricultural Soils." *Applied and Environmental Microbiology* 82 (10): 2919–28.

Homyak, Peter M., Joseph C. Blankinship, Kenneth Marchus, Delores M. Lucero, James O. Sickman, and Joshua P. Schimel. 2016. "Aridity and Plant Uptake Interact to Make Dryland Soils Hotspots for Nitric Oxide (NO) Emissions." *Proceedings of the National Academy of Sciences* 113 (19): E2608–16.

Homyak, Peter M., Matthew Kamiyama, James O. Sickman, and Joshua P. Schimel. 2017. "Acidity and Organic Matter Promote Abiotic Nitric Oxide Production in Drying Soils." *Global Change Biology* 23 (4): 1735–47.

Huang, Ying, Jinquan Jing, Meiling Yan, Christina Hazard, Yuehong Chen, Chengbao Guo, Xu Xiao, and Jiujun Lin. 2021. "Contribution of Pathogenic Fungi to N2O Emissions Increases Temporally in Intensively Managed Strawberry Cropping Soil." *Applied Microbiology and Biotechnology* 105 (5): 2043–56.

Hungate, Bruce A., Rebecca L. Mau, Egbert Schwartz, J. Gregory Caporaso, Paul Dijkstra, Natasja van Gestel, Benjamin J. Koch, et al. 2015. "Quantitative Microbial Ecology through Stable Isotope Probing." *Applied and Environmental Microbiology* 81 (21): 7570–81.

Jenerette, G. Darrel, and Amitava Chatterjee. 2012. "Soil Metabolic Pulses: Water, Substrate, and Biological Regulation." *Ecology* 93 (5): 959–66.

Jia, Meiqing, Zhiwei Gao, Huijun Gu, Chenyu Zhao, Meiqi Liu, Fanhui Liu, Lina Xie, et al. 2021. “Effects of Precipitation Change and Nitrogen Addition on the Composition, Diversity, and Molecular Ecological Network of Soil Bacterial Communities in a Desert Steppe.” *PloS One* 16 (3): e0248194.

Kim, Sang-Wan, Shinya Fushinobu, Shengmin Zhou, Takayoshi Wakagi, and Hirofumi Shoun. 2009. “Eukaryotic nirK Genes Encoding Copper-Containing Nitrite Reductase: Originating from the Protomitochondrion?” *Applied and Environmental Microbiology* 75 (9): 2652–58.

Koch, Benjamin J., Theresa A. McHugh, Michaela Hayer, Egbert Schwartz, Steven J. Blazewicz, Paul Dijkstra, Natasja van Gestel, et al. 2018. “Estimating Taxon-Specific Population Dynamics in Diverse Microbial Communities.” *Ecosphere* 9 (1): e02090.

Koch, Hanna, Maartje A. H. J. van Kessel, and Sebastian Lücker. 2019. “Complete Nitrification: Insights into the Ecophysiology of Comammox Nitrospira.” *Applied Microbiology and Biotechnology* 103 (1): 177–89.

Kowalchuk, George A., and John R. Stephen. 2003. “Ammonia-Oxidizing Bacteria: A Model for Molecular Microbial Ecology,” November. https://doi.org/10.1146/annurev.micro.55.1.485.

Krichels, Alexander H., Peter M. Homyak, Emma L. Aronson, James O. Sickman, Jon Botthoff, Hannah Shulman, Stephanie Piper, Holly M. Andrews, and G. Darrel Jenerette. 2022. “Rapid Nitrate Reduction Produces Pulsed NO and N2O Emissions Following Wetting of Dryland Soils.” *Biogeochemistry* 158 (2): 233–50.

Kumar, Prasann, and Shweta Pathak. 2018. “Nitric Oxide: A Key Driver of Signaling in Plants.” *MOJ Ecology & Environmental Sciences* 3 (3). https://doi.org/10.15406/mojes.2018.03.00079.

Kuypers, Marcel M. M., Hannah K. Marchant, and Boran Kartal. 2018. “The Microbial Nitrogen-Cycling Network.” *Nature Reviews. Microbiology*, February. https://doi.org/10.1038/nrmicro.2018.9.

Lauber, Christian L., Micah Hamady, Rob Knight, and Noah Fierer. 2009. “Pyrosequencing-Based Assessment of Soil pH as a Predictor of Soil Bacterial Community Structure at the Continental Scale.” *Applied and Environmental Microbiology* 75 (15): 5111–20.

Laughlin, R. J., and R. J. Stevens. 2002. “Evidence for Fungal Dominance of Denitrification and Codenitrification in a Grassland Soil.” *Soil Science Society of America Journal. Soil Science Society of America*. https://acsess.onlinelibrary.wiley.com/doi/abs/10.2136/sssaj2002.1540.

Lee, Xuhui, Hui-Ju Wu, Jeffrey Sigler, Christopher Oishi, and Thomas Siccama. 2004. “Rapid and Transient Response of Soil Respiration to Rain.” *Global Change Biology* 10 (6): 1017–26.

Leitner, S., P. M. Homyak, and J. C. Blankinship. 2017. “Linking NO and N2O Emission Pulses with the Mobilization of Mineral and Organic N upon Rewetting Dry Soils.” *Soil Biology and*. https://www.sciencedirect.com/science/article/pii/S0038071717305709.

Lester, Elizabeth D., Masataka Satomi, and Adrian Ponce. 2007. “Microflora of Extreme Arid Atacama Desert Soils.” *Soil Biology & Biochemistry* 39 (2): 704–8.

Lin, Huang, and Shyamal Das Peddada. 2020a. “Analysis of Compositions of Microbiomes with Bias Correction.” *Nature Communications* 11 (1): 3514.

———. 2020b. “Analysis of Microbial Compositions: A Review of Normalization and Differential Abundance Analysis.” *Npj Biofilms and Microbiomes* 6 (1): 1–13.

Luque-Almagro, Víctor M., Andrew J. Gates, Conrado Moreno-Vivián, Stuart J. Ferguson, David J. Richardson, and M. Dolores Roldán. 2011. “Bacterial Nitrate Assimilation: Gene Distribution and Regulation.” *Biochemical Society Transactions* 39 (6): 1838–43.

Maia, Luisa B., and José J. G. Moura. 2014. “How Biology Handles Nitrite.” *Chemical Reviews* 114 (10): 5273–5357.

Maier, S., A. M. Kratz, J. Weber, M. Prass, F. Liu, A. T. Clark, R. M. M. Abed, et al. 2022. “Water-Driven Microbial Nitrogen Transformations in Biological Soil Crusts Causing Atmospheric Nitrous Acid and Nitric Oxide Emissions.” *The ISME Journal* 16 (4): 1012–24.

Marcos, Ana T., María S. Ramos, Jose F. Marcos, Lourdes Carmona, Joseph Strauss, and David Cánovas. 2016. “Nitric Oxide Synthesis by Nitrate Reductase Is Regulated during Development in Aspergillus.” *Molecular Microbiology* 99 (1): 15–33.

Massimo, Nicholas C., M. M. Nandi Devan, Kayla R. Arendt, Margaret H. Wilch, Jakob M. Riddle, Susan H. Furr, Cole Steen, Jana M. U’Ren, Dustin C. Sandberg, and A. Elizabeth Arnold. 2015. “Fungal Endophytes in Aboveground Tissues of Desert Plants: Infrequent in Culture, but Highly Diverse and Distinctive Symbionts.” *Microbial Ecology* 70 (1): 61–76.

McMurdie, Paul J., and Susan Holmes. 2013. “Phyloseq: An R Package for Reproducible Interactive Analysis and Graphics of Microbiome Census Data.” *PloS One* 8 (4): e61217.

Mohan, Schmid, and Jetten. 2004. “Detection and Widespread Distribution of the nrfA Gene Encoding Nitrite Reduction to Ammonia, a Short Circuit in the Biological Nitrogen Cycle That Competes with ….” *FEMS Microbiology Ecology*. https://academic.oup.com/femsec/article-abstract/49/3/433/585024.

Morrissey, Ember M., Rebecca L. Mau, Egbert Schwartz, Benjamin J. Koch, Michaela Hayer, and Bruce A. Hungate. 2018. “Taxonomic Patterns in the Nitrogen Assimilation of Soil Prokaryotes.” *Environmental Microbiology* 20 (3): 1112–19.

Mothapo, Nape, Huaihai Chen, Marc A. Cubeta, Julie M. Grossman, Fred Fuller, and Wei Shi. 2015. “Phylogenetic, Taxonomic and Functional Diversity of Fungal Denitrifiers and Associated N2O Production Efficacy.” *Soil Biology & Biochemistry* 83 (April): 160–75.

Nadeau, Sarah A., Constance A. Roco, Spencer J. Debenport, Todd R. Anderson, Kathryn L. Hofmeister, M. Todd Walter, and James P. Shapleigh. 2019. “Metagenomic Analysis Reveals Distinct Patterns of Denitrification Gene Abundance across Soil Moisture, Nitrate Gradients.” *Environmental Microbiology* 21 (4): 1255–66.

Palmer, Jonathan M., Michelle A. Jusino, Mark T. Banik, and Daniel L. Lindner. 2018. “Non-Biological Synthetic Spike-in Controls and the AMPtk Software Pipeline Improve Mycobiome Data.” *PeerJ* 6 (May): e4925.

Pandey, C. B., Upendra Kumar, Megha Kaviraj, K. J. Minick, A. K. Mishra, and J. S. Singh. 2020. “DNRA: A Short-Circuit in Biological N-Cycling to Conserve Nitrogen in Terrestrial Ecosystems.” *The Science of the Total Environment* 738 (October): 139710.

Parker, Sophie S., and Joshua P. Schimel. 2011. “Soil Nitrogen Availability and Transformations Differ between the Summer and the Growing Season in a California Grassland.” *Applied Soil Ecology: A Section of Agriculture, Ecosystems & Environment* 48 (2): 185–92.

Patro, Rob, Geet Duggal, Michael I. Love, Rafael A. Irizarry, and Carl Kingsford. 2017. “Salmon Provides Fast and Bias-Aware Quantification of Transcript Expression.” *Nature Methods* 14 (4): 417–19.

Pessi, Igor S., Sirja Viitamäki, Eeva Eronen-Rasimus, Tom O. Delmont, Miska Luoto, and Jenni Hultman. 2020. “Truncated Denitrifiers Dominate the Denitrification Pathway in Tundra Soil Metagenomes.” *Cold Spring Harbor Laboratory*. https://doi.org/10.1101/2020.12.21.419267.

Placella, Sarah Anne. 2011. “Gene Expression by Microbial Communities in Response to Soil Wet-Up: Microbial Resuscitation Strategies, Nitrifier Response Dynamics, and N2O Pulses.” UC Berkeley. https://escholarship.org/uc/item/91048093.

Putz, Martina, Philipp Schleusner, Tobias Rütting, and Sara Hallin. 2018. “Relative Abundance of Denitrifying and DNRA Bacteria and Their Activity Determine Nitrogen Retention or Loss in Agricultural Soil.” *Soil Biology & Biochemistry* 123 (August): 97–104.

Quast, Christian, Elmar Pruesse, Pelin Yilmaz, Jan Gerken, Timmy Schweer, Pablo Yarza, Jörg Peplies, and Frank Oliver Glöckner. 2013. “The SILVA Ribosomal RNA Gene Database Project: Improved Data Processing and Web-Based Tools.” *Nucleic Acids Research* 41 (Database issue): D590–96.

Ramond, Jean-Baptiste, Karen Jordaan, Beatriz Díez, Sandra M. Heinzelmann, and Don A. Cowan. 2022. “Microbial Biogeochemical Cycling of Nitrogen in Arid Ecosystems.” *Microbiology and Molecular Biology Reviews: MMBR*, April, e0010921.

Rao, Leela E., and Edith B. Allen. 2010. “Combined Effects of Precipitation and Nitrogen Deposition on Native and Invasive Winter Annual Production in California Deserts.” *Oecologia* 162 (4): 1035–46.

Rao, L. E., D. R. Parker, A. Bytnerowicz, and E. B. Allen. 2009. “Nitrogen Mineralization across an Atmospheric Nitrogen Deposition Gradient in Southern California Deserts.” *Journal of Arid Environments* 73 (10): 920–30.

Ridenhour, Benjamin J., Sarah L. Brooker, Janet E. Williams, James T. Van Leuven, Aaron W. Miller, M. Denise Dearing, and Christopher H. Remien. 2017. “Modeling Time-Series Data from Microbial Communities.” *The ISME Journal* 11 (11): 2526–37.

Schaeffer, S. M., S. A. Billings, and R. D. Evans. 2003. “Responses of Soil Nitrogen Dynamics in a Mojave Desert Ecosystem to Manipulations in Soil Carbon and Nitrogen Availability.” *Oecologia* 134 (4): 547–53.

Schimel, J., T. C. Balser, and M. Wallenstein. 2007. “Microbial Stress‐response Physiology and Its Implications for Ecosystem Function.” *Ecology*. https://agupubs.onlinelibrary.wiley.com/doi/abs/10.1890/06-0219.

Schimel, J. P., J. Å. M. Wetterstedt, and P. A. Holden. 2011. “Drying/rewetting Cycles Mobilize Old C from Deep Soils from a California Annual Grassland.” *Soil Biology and*. https://www.sciencedirect.com/science/article/pii/S0038071711000228.

Schinko, Thorsten, Harald Berger, Wanseon Lee, Andreas Gallmetzer, Katharina Pirker, Robert Pachlinger, Ingrid Buchner, Thomas Reichenauer, Ulrich Güldener, and Joseph Strauss. 2010. “Transcriptome Analysis of Nitrate Assimilation in Aspergillus Nidulans Reveals Connections to Nitric Oxide Metabolism.” *Molecular Microbiology* 78 (3): 720–38.

Shade, Ashley, J. Gregory Caporaso, Jo Handelsman, Rob Knight, and Noah Fierer. 2013. “A Meta-Analysis of Changes in Bacterial and Archaeal Communities with Time.” *The ISME Journal* 7 (8): 1493–1506.

Shoun, Hirofumi, Shinya Fushinobu, Li Jiang, Sang-Wan Kim, and Takayoshi Wakagi. 2012. “Fungal Denitrification and Nitric Oxide Reductase Cytochrome P450nor.” *Philosophical Transactions of the Royal Society of London. Series B, Biological Sciences* 367 (1593): 1186–94.

Shoun, H., and T. Tanimoto. 1991. “Denitrification by the Fungus Fusarium Oxysporum and Involvement of Cytochrome P-450 in the Respiratory Nitrite Reduction.” *The Journal of Biological Chemistry* 266 (17): 11078–82.

Slessarev, Eric W., Aral C. Greene, Peter M. Homyak, Samantha C. Ying, and Joshua P. Schimel. 2021. “High Resolution Measurements Reveal Abiotic and Biotic Mechanisms of Elevated Nitric Oxide Emission after Wetting Dry Soil.” *Soil Biology & Biochemistry* 160 (September): 108316.

Stein, Lisa Y. 2011. “Surveying N2O-Producing Pathways in Bacteria.” *Methods in Enzymology* 486: 131–52.

———. 2017. “Resolving N2 O Respiration Pathways: A Tale of Two NosZ Clades.” *Environmental Microbiology*.

Thomson, Andrew J., Georgios Giannopoulos, Jules Pretty, Elizabeth M. Baggs, and David J. Richardson. 2012. “Biological Sources and Sinks of Nitrous Oxide and Strategies to Mitigate Emissions.” *Philosophical Transactions of the Royal Society of London. Series B, Biological Sciences* 367 (1593): 1157–68.

Timmis, Jeremy N., Michael A. Ayliffe, Chun Y. Huang, and William Martin. 2004. “Endosymbiotic Gene Transfer: Organelle Genomes Forge Eukaryotic Chromosomes.” *Nature Reviews. Genetics* 5 (2): 123–35.

Trost, Benjamin, Annette Prochnow, Katrin Drastig, Andreas Meyer-Aurich, Frank Ellmer, and Michael Baumecker. 2013. “Irrigation, Soil Organic Carbon and N2O Emissions. A Review.” *Agronomy for Sustainable Development* 33 (4): 733–49.

Tu, Qichao, Lu Lin, Lei Cheng, Ye Deng, and Zhili He. 2018. “NCycDB: A Curated Integrative Database for Fast and Accurate Metagenomic Profiling of Nitrogen Cycling Genes.” *Bioinformatics* , August. https://doi.org/10.1093/bioinformatics/bty741.

Unger, Stephan, Cristina Máguas, João S. Pereira, Teresa S. David, and Christiane Werner. 2010. “The Influence of Precipitation Pulses on Soil Respiration – Assessing the ‘Birch Effect’ by Stable Carbon Isotopes.” *Soil Biology & Biochemistry* 42 (10): 1800–1810.

Uritskiy, Gherman V., Jocelyne DiRuggiero, and James Taylor. 2018. “MetaWRAP-a Flexible Pipeline for Genome-Resolved Metagenomic Data Analysis.” *Microbiome* 6 (1): 158.

Vázquez, Eduardo, Nikola Teutscherova, Roberta Pastorelli, Alessandra Lagomarsino, Laura Giagnoni, and Giancarlo Renella. 2020. “Liming Reduces N2O Emissions from Mediterranean Soil after-Rewetting and Affects the Size, Structure and Transcription of Microbial Communities.” *Soil Biology & Biochemistry* 147 (August): 107839.

Vázquez-Torres, Andrés, and Andreas J. Bäumler. 2016. “Nitrate, Nitrite and Nitric Oxide Reductases: From the Last Universal Common Ancestor to Modern Bacterial Pathogens.” *Current Opinion in Microbiology* 29 (February): 1–8.

Vourlitis, George L., Karri Kirby, Issac Vallejo, Jacob Asaeli, and Joshua M. Holloway. 2021. “Potential Soil Extracellular Enzyme Activity Is Altered by Long-Term Experimental Nitrogen Deposition in Semiarid Shrublands.” *Applied Soil Ecology: A Section of Agriculture, Ecosystems & Environment* 158 (February): 103779.

Vuono, David C., Robert W. Read, James Hemp, Benjamin W. Sullivan, John A. Arnone 3rd, Iva Neveux, Robert R. Blank, et al. 2019. “Resource Concentration Modulates the Fate of Dissimilated Nitrogen in a Dual-Pathway Actinobacterium.” *Frontiers in Microbiology* 10 (January): 3.

Wang, H., and R. P. Gunsalus. 2000. “The nrfA and nirB Nitrite Reductase Operons in Escherichia Coli Are Expressed Differently in Response to Nitrate than to Nitrite.” *Journal of Bacteriology* 182 (20): 5813–22.

Wang, Zhen, Risu Na, Liz Koziol, Michael P. Schellenberg, Xiliang Li, Na Ta, Ke Jin, and Hai Wang. 2020. “Response of Bacterial Communities and Plant-Mediated Soil Processes to

Nitrogen Deposition and Precipitation in a Desert Steppe." *Plant and Soil* 448 (1): 277–97.

Wolińska, A., A. Kuźniar, U. Zielenkiewicz, and A. Banach. 2018. "Indicators of Arable Soils fatigue–Bacterial Families and Genera: A Metagenomic Approach." *Ecological*. https://www.sciencedirect.com/science/article/pii/S1470160X18303753?casa_token=5aoXgNio81wAAAAA:rYrFMq6iNnT4WxDd_nQ5ZnjyfF-9oUP2oIZoMFEouXJ3BY7ethVFR5elDv05Rbt3Ui96dD7F.

Yoon, Sukhwan, Bongkeun Song, Rebecca L. Phillips, Jin Chang, and Min Joon Song. 2019. "Ecological and Physiological Implications of Nitrogen Oxide Reduction Pathways on Greenhouse Gas Emissions in Agroecosystems." *FEMS Microbiology Ecology* 95 (6). https://doi.org/10.1093/femsec/fiz066.

Zaady, Eli. 2005. "Seasonal Change and Nitrogen Cycling in a Patchy Negev Desert: A Review." *Arid Land Research and Management* 19 (2): 111–24.

Zhang, Bingchang, Weidong Kong, Nan Wu, and Yuanming Zhang. 2016. "Bacterial Diversity and Community along the Succession of Biological Soil Crusts in the Gurbantunggut Desert, Northern China." *Journal of Basic Microbiology* 56 (6): 670–79.

Zhang, Tian 'an, Han Y. H. Chen, and Honghua Ruan. 2018. "Global Negative Effects of Nitrogen Deposition on Soil Microbes." *The ISME Journal*, March. https://doi.org/10.1038/s41396-018-0096-y.

Zhao, Yanxia, Jieyin Lim, Jianyang Xu, Jae-Hyuk Yu, and Weifa Zheng. 2020. "Nitric Oxide as a Developmental and Metabolic Signal in Filamentous Fungi." *Molecular Microbiology* 113 (5): 872–82.